

BATES, GINGER MUSE. Characterization of the protein component of *Methanococcus jannaschii* RNase P. (Under the direction of James W. Brown.)

RNase P is the ribonuclease responsible for the 5' maturation of precursor transfer RNA (pre-tRNA). In Bacteria RNase P is composed of a single 14kDa protein accompanied by a single catalytic RNA subunit that is capable of cleave pre-tRNA without the protein cofactor *in vitro*. The RNA subunit of archaeal RNase P resembles those found in Bacteria, however holoenzymes characterized from the Archaea indicate that the accompanying protein component is much larger than in the bacterial enzyme. Purified RNase P from the Euryarchaeon *Methanococcus jannaschii* possesses approximately eight protein subunits and has an RNA that is incapable of cleaving pre-tRNA alone *in vitro*. Four putative *M. jannaschii* RNase P proteins have been identified by their similarity to RNase P proteins of *Methanothermobacter thermoautotrophicus*. Here we confirm the presence of two of these proteins, MJ0464 and MJ1139, as well as the presence of several other hypothetical proteins (MJ0332.1, MJ0376, MJ1128, and MJ1625), two 30S ribosomal protein subunits (S6E and S8E), and a nicotinamide-nucleotide adenylyltransferase in *M. jannaschii* RNase P preparations. Eukaryotic RNase P holoenzymes also contain multiple protein subunits and it is thought that these "extra" proteins are required for function in the increased compartmentalization of the eukaryotic cell. Archaeal cells do not have the distinct compartmentalization seen in eukaryotic cells and it is unclear what purpose the protein subunits described here would have *in vivo*. One possibility is protein-substrate interactions to facilitate formation of the substrate-enzyme complex. *M. jannaschii* RNase P RNA lacks certain secondary structures present in *E. coli* RNase P RNA that have been shown in the bacterial model to interact with pre-tRNA substrate. Archaeal RNase P RNAs that possess these elements, such as that of M.

thermoautotrophicus, are capable of cleaving substrate in vitro without protein, although only at very high salt concentration. *M. jannaschii* RNase P RNA does not have any extra secondary structural elements to compensate for the lack of substrate binding helices and it is possible that the protein component has evolved to assume these responsibilities. In order to test this hypothesis, circularly permuted transfer RNAs containing a photoagent positioned in the T loop were used in ultra-violet cross-linking reactions.

**CHARACTERIZATION OF THE PROTEIN COMPONENT OF
METHANOCOCCUS JANNASCHII RNASE P**

by

GINGER M. BATES

A thesis submitted to the Graduate Faculty of
the North Carolina State University
in partial fulfillment of the
requirements for the Degree of
Master of Science

MICROBIOLOGY

Raleigh

2001

APPROVED BY:

Chair of Advisory Committee

ACKNOWLEDGEMENTS

Without the support of friends, family and colleagues I probably wouldn't have made it as far as this. I would like to thank all of you who have supported me through my endeavors and opened doors that otherwise would have remained closed. I give special thanks to Dr. Jim Brown for giving me a place to explore knowledge and all of the Brown Lab members for providing much appreciated help along the way. I thank my parents for birthing and loving me, other members of the NCSU Microbiology graduate program for commiserating with me, and my committee members, Dr. Steve Libby and Dr. Amy Grunden along with Dr. Jim Brown, for approving the following thesis work.

BIOGRAPHY

Ginger Muse Bates was born October 11, 1976 in Asheville, North Carolina to Alan and Jeanne Muse. She spent seventeen years of life in western North Carolina and graduated from T. C. Roberson High School in 1994. Graduating from North Carolina State University with a Bachelors of Science in Microbiology, a Minor in Genetics, and a Minor in Horticulture, she continued her education to complete a Master of Science in Microbiology also at North Carolina State University. Upon completion of the following thesis work she accepted a position working for the Howard Hughes Medical Institute at Duke University, Durham, NC. Her current research focuses on using retroviruses to study eukaryotic messenger RNA transport.

TABLE OF CONTENTS

List of Tables	v
List of Figures	vi
RNase P Review	1
RNA structure and function	1
The RNase P reaction	3
Bacterial RNase P	5
Archaeal RNase P	7
Nuclear RNase P	9
Organellar RNase P	10
References	18
Chapter 1: Identification of substrate-holoenzyme interactions in <i>Methanococcus jannaschii</i> RNase P	23
Abstract	23
Introduction	25
Materials and Methods	28
Results and Discussion	30
References	36
Chapter 2: Purification and characterization of RNase P protein subunits from <i>Methanococcus jannaschii</i>	38
Abstract	38
Introduction	40
Materials and Methods	42
Results and Discussion	44
References	62
Appendix A: Cloning of the <i>Pyrococcus furiosus</i> DNA polymerase gene	64

LIST OF TABLES

Chapter 2: : Purification and characterization of RNase P protein subunits
from *Methanococcus jannaschii*

Table I. Summary of the mass spectrometry analysis of proteins purified from <i>M. jannaschii</i> RNase P	49
--	----

LIST OF FIGURES

RNase P Review

Figure 1: RNase P RNA consensus secondary structures for each domain of life	12
Figure 2: The RNase P RNA secondary structure for Micro P	13
Figure 3: The RNase P reaction	14
Figure 4: Examples of type A and type B bacterial RNase P RNA secondary structures	15
Figure 5: Examples of type A and type M achaeal RNase P RNA secondary structures	16
Figure 6: Examples of nuclear RNase P RNA secondary structure	17
Chapter 1: Identification of substrate-holoenzyme interactions in <i>Methanococcus jannaschii</i> RNase P	
Figure 1: Examples of type A and type M achaeal RNase P RNA secondary structures	33
Figure 2: Secondary structure of a circularly permuted transfer RNA	34
Figure 3: Crosslinking gel	35
Chapter 2: Purification and characterization of RNase P protein subunits from <i>Methanococcus jannaschii</i>	
Figure 1: RNase P activity assays	50
Figure 2: Glycerol gradient fractions exhibiting RNase P activity	51
Figure 3: SDS-PAGE analysis of active pooled glycerol gradient fractions	52
Figure 4: MALDI-TOF peptide mass finger print spectrum of the trypsin digest of gel slice MJ-2	53
Figure 5: MALDI-TOF peptide mass finger print spectrum of the trypsin digest of gel slice MJ-3	54
Figure 6: MALDI-TOF peptide mass finger print spectrum of the trypsin digest of gel slice MJ-4	55
Figure 7: MALDI-TOF peptide mass finger print spectrum of the trypsin digest of gel slice MJ-8	56
Figure 8: MALDI-TOF peptide mass finger print spectrum of the trypsin digest of gel slice MJ-9	57
Figure 9: MALDI-TOF peptide mass finger print spectrum of the trypsin digest of gel slice MJ-10	58
Figure 10: MALDI-TOF peptide mass finger print spectrum of the trypsin digest of gel slice MJ-12	59
Figure 11: MALDI-TOF peptide mass finger print spectrum of the trypsin digest of gel slice MJ-13	60
Figure 12: MALDI-TOF peptide mass finger print spectrum of the trypsin digest of gel slice MJ-14	61
Appendix A: Cloning of the <i>Pyrococcus furiosus</i> DNA polymerase gene	
Figure 1: PCR assay for polymerase activity	68

RNASE P REVIEW

In order for protein synthesis to occur, transfer RNAs generated in a precursor form (pre-tRNA) must undergo both 3' and 5' end processing to become the mature tRNAs utilized by the other tRNA processing machinery and finally the ribosome (59). The enzyme responsible for 5' cleavage of pre-tRNAs is ribonuclease P (RNase P), a ubiquitous and essential endoribonuclease (17,56). RNase Ps have been characterized from individuals of all three domains of life as well as from eukaryotic organelles (50). All RNase Ps characterized from eukaryotic nucleus, Bacteria, and Archaea consist of an RNA subunit and a protein component, the latter of which varies significantly between Domains. RNase P is unconventional in that the RNA subunit is the catalytic portion of the enzyme (19). All Bacteria and some of the Euryarchaea possess RNase Ps in which the RNA alone can cleave pre-tRNA *in vitro* (44). Though no RNAs isolated from the Eukarya exhibit this *in vitro* activity, it is still accepted that the RNA is catalytic *in vivo* (6). The *in vitro* activity along with the fact that RNase P RNA can catalyze multiple turnover events without loss of structure and function makes the enzyme a true ribozyme.

RNA Structure and Function

The RNase P RNAs have been characterized from organisms representing all domains of life. Of these, the bacterial RNAs, from *Escherichia coli* and *Bacillus subtilis* specifically, have been characterized extensively and much of the data concerning RNase P structure and function has come from these organisms. 3-D structures have been unattainable for the RNA or the holoenzyme from any organism. Several approaches to determine the secondary structures of these RNAs have been used including minimum

energy calculation, structure probing, enzymatic and chemical methods, and comparative sequence analysis (4,6,25). Of all of these, the last has proved to be the most powerful tool in resolving the secondary structure of RNase P RNAs and bacterial and archaeal secondary structures have been determined (21, 20, 24). Over 500 RNase P RNA sequences can be found listed phylogenetically on the RNase P database at <http://www.mbio.ncsu.edu/RNaseP> (3). The consensus secondary structures for the Archaea, Bacteria, and the Eukarya can be seen in Figure 1.

The secondary structures determined consist of a series of helices and loops numbered P1 through P21 according to their placement in the bacterial consensus sequence. A multitude of experiments support that P4 is the active site of the RNase P RNA and a conserved catalytic core has been diagrammed (Figure 1) (2,7,9,15,18,22,26,52). This correlates with the sequence conservation in this region, 11 nucleotides of the 21 that are absolutely conserved in P4 (16). All RNase P RNAs characterized thus far from the Archaea, Bacteria, and Eukarya contain helix P4 (60). More evidence to support P4 as the catalytic helix of RNase P is found in the secondary structure of Micro P (Figure 2), a synthetic RNase P RNA designed from the RNA of *Mycoplasma fermentans* and modified to only include helices absolutely required for catalytic activity. This RNase P RNA represents the smallest active RNase P RNA, containing the only P7-P10 cruciform structure, P1-P4, P5, and P15 (51). Recent data has revealed that the RNase P of *B. subtilis* can be separated into domains such as those seen in typical protein enzymes (37). In the case of *B. subtilis* RNase P, only the lower portion (P1 through P7) of the RNase P RNA accompanied by its protein cofactor is required to cleave a variety of substrates *in vitro* (37). As expected, this portion of

RNA contains all the elements predicted to be in the catalytic core, including the P4 region. Other regions of the bacterial RNA present are the L15 loop adjacent to the P15 helix implicated to play a role in substrate binding through modification experiments (8,52).

The RNase P Reaction

RNase P has the ability to cleave a wide range of substrates whether they are natural, such as hundreds of pre-tRNAs, SRP RNA, mRNA, and 4.5S RNA, or other substrates such as synthetic double stranded DNA, small synthetic RNAs, or circularly permuted tRNAs (10,11,36,37,42). Some evidence suggests that RNase P cleaves its own precursor RNA autolytically (36). Whatever the substrate, the RNase P reaction can be described in three steps: (1) Formation of the enzyme-substrate complex, (2) hydrolysis of the scissile phosphodiester bond, and (3) dissociation of reaction products (60).

Among the naturally occurring substrates, pre-tRNAs carry few common sequences among them that would allow recognition by RNase P for substrate binding through Watson-Crick base pairing (43). The enzyme rather seems to recognize the three dimensional tertiary structure presented by the acceptor stem, T loop, and T arm folded into the L-shaped conformation (Figure 3) (4,23,27,41). The conserved 3' "NCCA" tail of the tRNA has been implicated in positioning the reactive phosphodiester bond into the active site of RNase P by base pairing with the "GGU" sequence found in the loop joining P15 and P16 (labeled in Figure 4) (32). Other evidence suggests that the 5' leader sequence is required for proper placement of the tRNA in the RNase P active site (8,35,58). This second notion is supported by instances where either the RNase P RNA

lacks the GGU motif, such as in the cyanobacteria where the RNA is catalytic alone in vitro, or the tRNAs lack the 3'CCA tail such as in chloroplasts and other photosynthetic organisms (50). The RNase P protein also cross-links to the 5' leader sequence. NMR studies have shown that the base pairing interaction between pre-tRNA and RNase P RNA is probable, however kinetic experiments indicate that it facilitates binding but is not necessary for binding.

The physical cleavage by RNase P of the pre-tRNA 5' leader is a hydrolytic reaction where a water molecule activated by Mg^{2+} attacks the scissile phosphodiester bond resulting in a 3' hydroxyl on the leader and a 5' phosphate on the tRNA (42). The resulting mature tRNA can then participate in other modification procedures and eventually participate in protein synthesis. This reaction is dependant on cations, monovalent for shielding of the negative phosphate backbones of both substrate and enzyme, and divalent cations to maintain structure and for catalysis (49). RNase P prefers Mg^{2+} , although other cations such as Ca^{2+} and Mn^{2+} can be utilized with lower catalytic efficiency (17). Three Mg^{2+} ions are thought to be coordinated for catalysis forming a trigonal bipyramid illustrated in Figure 3 (6,42,53,54). In Bacteria and the Eukarya, a phosphorothioate substitution at the scissile bond of the tRNA inhibits the 5' cleavage of tRNA (57). When Mn^{2+} , a cation that interacts more favorably with sulfur, is added to this reaction, cleavage proceeds. This supports the participation of Mg^{2+} at the scissile bond of the tRNA and the active site of RNase P. After cleavage of the scissile bond, the products of the reaction dissociate from the complex, the leader to be degraded and the mature tRNA to be further processed and utilized by the translation apparatus.

Bacterial RNase P

Most of the data concerning RNase P has been generated from the Bacteria, *E. coli* and *B. subtilis*. The RNase P RNA in Bacteria is ~300-400nts accompanied by a single 13-14kDa protein, both of which are essential *in vivo* (19). However, all Bacteria possess an RNase P with an RNA that is catalytic without protein *in vitro* (17).

The proteins identified from *B. subtilis* and *E. coli* are small basic proteins initially thought to merely provide electrostatic shielding since increasing the concentration of cations in the RNA-alone reaction compensates for the absence of protein (39,55). Since that initial hypothesis, several other roles for the protein cofactor of bacterial RNase P have been suggested (47). The C5 protein contacts the 5' leader of tRNA directly and has been shown to increase RNase P's affinity for pre-tRNA over mature tRNA (13,30). RNase T1 has an altered accessibility pattern when reacted with the holoenzyme as opposed to the RNA alone indicating that the C5 protein may loosen (or tighten) the RNA structure in order to facilitate product release (28,38,46). The protein has also been seen to alter RNase P substrate specificity to include 4.5S RNA, an RNA involved in protein secretion (45). None of the protein subunits in bacterial RNase P have identified RNA binding motifs. The crystal structure of the *B. subtilis* RNase P protein has been solved showing a cleft where a single stranded RNA can fit, presumably the 5' leader mentioned earlier, but the site of binding to RNase P RNA is not known.

Bacterial RNase P RNA is better understood than its protein cofactor, and while its 3-D structure has not been solved, the secondary structure is highly refined through comparative analysis of a large number of bacterial sequences, and a robust 3-D model

has been constructed (21, 60). The RNase P RNA secondary structures in Bacteria can be divided into two categories, the Low G+C Gram-positive Bacteria, such as *B. subtilis* and relatives, have type B RNAs, and all other bacterial RNAs fit into the ancestral type, or type A, RNAs (21). Figure 4 shows the RNA secondary structures for *E. coli*, representing type A (the ancestral type), and *B. subtilis*, representing type B, or *Bacillus* like. Though the secondary structures of these two distinct types of RNAs have many obvious differences, their kinetic properties are very similar and they can utilize each other's proteins *in vitro* indicating that in three-dimensional space they have much in common (21).

Type A RNAs are found in the majority of Bacteria and the numbering of the *E. coli* RNase P RNA is the basis for the numbering of all RNase P RNA structures. Helices are indicated by the letter "P" and are numbered consecutively while the unpaired regions between helices are indicated by the letter "J" and the numbers of the neighboring helices. Loops terminating helices are indicated by an "L" and the helix number. *E. coli* RNase P RNA has 18 helices, including the pseudoknot P6 and the catalytic helix P4. As mentioned previously, P8, P9 and J15/16 interact with pre-tRNA substrate.

Type B RNAs contain the conserved core essential for catalysis however they have altered tertiary interactions that are thought to mimic the ones found in the ancestral RNAs. One example of this is the missing P6 and P17 pseudoknot, which is thought to be replaced by P5.1 in type B RNAs (21). Covariation between nucleotide A71 in this L5.1 and U283 in L15.1 support this interaction. What prompted the sudden change in RNase P RNA structures found in the gram positive bacteria is unknown.

Archaeal RNase P

Archaeal RNase P is less understood than its bacterial counterparts due to a number of scientific difficulties. Many Archaea are difficult to cultivate, especially in large batch culture, and a robust genetic system has yet to be developed in Archaea. Until recently, the only RNase P holoenzymes characterized from Archaea were those of two distantly related organisms, in the Euryarchaea the extreme halophile *Haloferax volcanii* and in the Crenarchaea the thermophilic sulfur oxidizing *Sulfolobus acidocaldarius* (33). The findings from these purified enzymes indicated that the Archaea may harbor a wide variety of RNase Ps among them. The RNase P from *H. volcanii* has a buoyant density in Cs_2SO_4 of 1.59g/ml, close to that of RNA alone, and is highly sensitive to nuclease treatment, whereas the holoenzyme from *S. acidocaldarius* has a buoyant density of 1.27g/ml suggesting that it is largely made of protein and is insensitive to nuclease treatment (14,33). These two very different RNase Ps by themselves seem to represent a diverse group of RNase P RNAs among the Archaea. Recently RNase Ps from two methanogenic Archaea, *Methanothermobacter thermoautotrophicus* (formerly known as *Methanobacterium thermoautotrophicum* ΔH) and *Methanococcus jannaschii*, have been purified and characterized (1). The characteristics of these two holoenzymes indicate that RNase Ps among the Archaea may have more in common than previously thought. Both RNase Ps have buoyant densities in the median between that of protein and RNA (1.39g/ml for *M. jannaschii* RNase P and 1.42g/ml for *M. thermoautotrophicus* RNase P) (1).

The RNA subunits from archaeal RNase Ps resemble the bacterial ancestral type secondary structure. All archaeal RNase P RNAs lack helices P13/14 and P18 (20,24).

Although all bacterial RNase P RNAs have ribozyme activity *in vitro*, only some of the RNase P RNAs from the Archaea have activity without their proteins and only at very high ionic strength (44).

Like bacterial RNase P RNAs, archaeal RNase P RNAs can be categorized into two structural types. Type A, the ancestral type, is represented by *M. thermoautotrophicus* in Figure 5 along with that of *M. jannaschii* representing the type M secondary structure. Some type A RNAs do possess ribozyme activity *in vitro*, but as mentioned, only at high ionic strength. This high salt requirement was presumed to be due to the absence of P18. Chimera experiments in which P18 was added to an archaeal type A RNA indicated that such was not the case (24). No type M RNAs have activity *in vitro* without their associated proteins. Type M RNAs differ in three major ways from type A RNAs, they lack elements P6, P8, and the L15/P16P/17 element. Of these three elements, P8 and the J15/16 junction between P15 and P16 have been shown to interact with pre-tRNA substrate. Cross-linking experiments using bacterial RNase P RNA indicate that residues in P8 bind residues in the Tloop of pre-tRNA (40) and the “GGU” motif in the J15/16 base-pairs to the 3' NCCA tail of pre-tRNA (32). Though type M RNAs lack key substrate binding motifs, and the tertiary interaction P6 formed by J5/7 and L17, the RNAs do not have any extra structure that could compensate for these functions. The inability to bind substrate, inability to form the correct tertiary structure, or both could result in the inactivity of type M RNAs. Since there are no extra structures in the type M RNAs, it is hypothesized that the additional protein subunits of these RNase Ps may have substrate binding roles.

The protein content of the archaeal RNase Ps is higher than seen in the bacterial holoenzyme and appears to resemble that of the eukaryotic RNase P protein component. Four proteins have been identified in the *M. jannaschii* and *M. thermoautotrophicus* genomes having similarity to RNase P proteins in *Saccharomyces cerevisiae* (Hall and Brown, submitted). These proteins also have obvious homologues in the genomes of other Archaea (29). Antiserum against the recombinant *M. thermoautotrophicus* proteins immunoprecipitates RNase P activity. Western blots also indicate that these proteins copurify with the RNase P holoenzyme of *M. thermoautotrophicus* (Hall and Brown, submitted).

Nuclear RNase P

RNase Ps from Eukarya have not been as extensively characterized as those in Bacteria, however the holoenzymes from both humans and yeast have been purified. Eukaryotic RNase P contains a single RNA subunit that is not catalytic *in vitro* in the absence of protein (6,60). These RNAs do have a secondary structure containing the conserved core domain. Although these RNAs are not competent *in vitro* without their associated proteins, it has been seen that these RNase Ps are sensitive to a phosphorothioate substitution at the scissile bond of tRNA, a characteristic seen previously in bacterial RNase Ps, and are the catalytic subunit of RNase P *in vivo* (57).

In *S. cerevisiae* this RNA, RPP1 has nine associated proteins (Pop1p Pop3p Pop4p Pop5p Pop6p Pop7p Pop8p, Rpp1p, and Rpr2p) identified by mass spectrometry and ranging 100kDa to 15kDa in molecular weight (5,60). Of these nine proteins, eight are shared by RNase MRP, a ribosomal RNA processing enzyme (5). RNase P RNA is also evolutionarily related to RNase MRP RNA. Several of the yeast RNase P proteins

also have homologues in human RNase P. It is hypothesized that the larger amount of protein in eukaryotic RNase Ps is needed for function in the increased organizational complexity of eukaryotic cells. Proposed functions for the additional RNase P protein subunits in eukaryotes are for translocation, protein mediated interactions and RNA binding. Human RNase P protein Rpp20 has been shown to have ATPase activity in the form of a DEAD box helicase motif seen in ABC transporters (34).

Organellar RNase P

Of all RNase Ps, those isolated from eukaryotic organelles are the most enigmatic, and much of the data concerning these enzymes is controversial. RNase Ps have been isolated and characterized from yeast and human mitochondria as well as from chloroplasts in both higher and lower photosynthetic Eukaryotes.

Mitochondrial RNase P from *S. cerevisiae* has an RNase P RNA and a 100 kDa protein (RPM1) encoded in the mitochondrial chromosome (48). The secondary structure of this RNA has been difficult to assess because of the AU richness of the sequence, however it potentially has a typical RNA secondary structure containing the conserved catalytic core. The RNA subunit from human mitochondria has not been firmly established yet. An RNA from human mitochondrial RNase P extracts has been isolated and characterized as having the exact same sequence as the nuclear RNase P RNA found in the same cells (60). No evidence has been provided that mitochondria can import an RNA of such size, and there is much debate as to whether this RNA is indeed mitochondrial RNase P or is nuclear contamination.

Photosynthetic organelles are derived from cyanobacteria and would be expected to resemble their bacterial counterparts in cellular components (50). This is true for

primitive plastids isolated from non-green algae but not true for chloroplasts of higher photosynthetic Eukaryotes (50). The RNase P RNA from cyanobacteria, like all bacterial RNase P RNAs, is a true ribozyme, however RNase P RNA from the *Cyanophora paradoxa* cyanelles is not (12). The protein of this RNase P has not been identified and it is hypothesized that the protein may be imported from the cytoplasm.

Data provided from analysis of the spinach chloroplast RNase P does not fit the usual situation for RNase P. Chloroplast RNase P isolated from spinach has a buoyant density in CsCl of 1.28g/ml, which is that of bulk protein and has an estimated size of 70kDa (57). The protein component of this ribonuclease can be fractionated into a 30kDa subunit and a 50kDa subunit. The enzyme is insensitive to micrococcal nuclease treatment and no RNA has been seen to associate with the protein. It is not clear whether or not spinach chloroplast RNase P has an RNA subunit (50). Even more interesting is that enzyme activity is not affected by the substitution of a phosphorothioate modification at the scissile bond of pre-tRNA (60). This indicates that this RNase P does not use the same cleavage mechanism described for that of eukaryotic and bacterial RNase Ps.

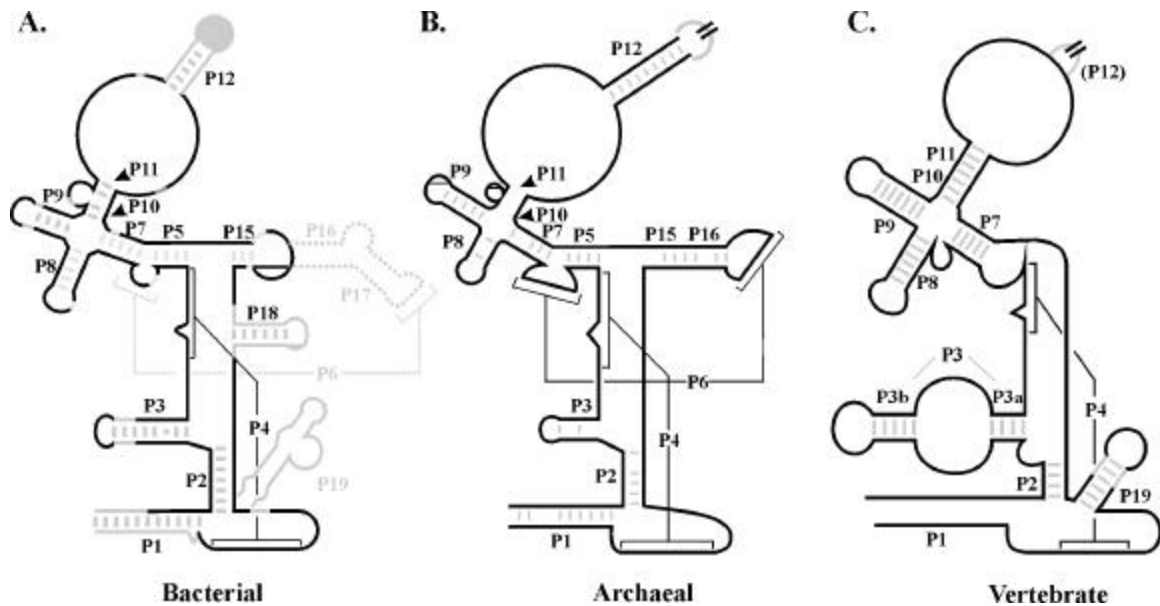


Figure 1. The consensus RNase P RNA secondary structures for each domain of life. Illustrated here are the consensus secondary structures in Bacteria (A), Archaea (B), and in vertebrate Eukaryotes (C). Portions of the RNA secondary structure that are 100% conserved are indicated by a solid black lines while portions that are conserved greater than 80% in Eukarya (c) and greater than 90% in Bacteria (b) are shown in gray. Only ancestral type (type A) structures are shown here for simplicity (a).

Figure 1 References:

- a. **Hall, T.**, Thesis
- b. **Brown, J.W.**. 1999. The ribonuclease P database. *Nucleic Acids Res.* 27:314
- c. **Pitulle, C., Garcia-Paris, M., Zamudio, K.R., and N.R. Pace.** 1999. Comparative structure analysis of vertebrate ribonuclease P RNA. *Nucleic Acids Res.* 26:3333-3339.

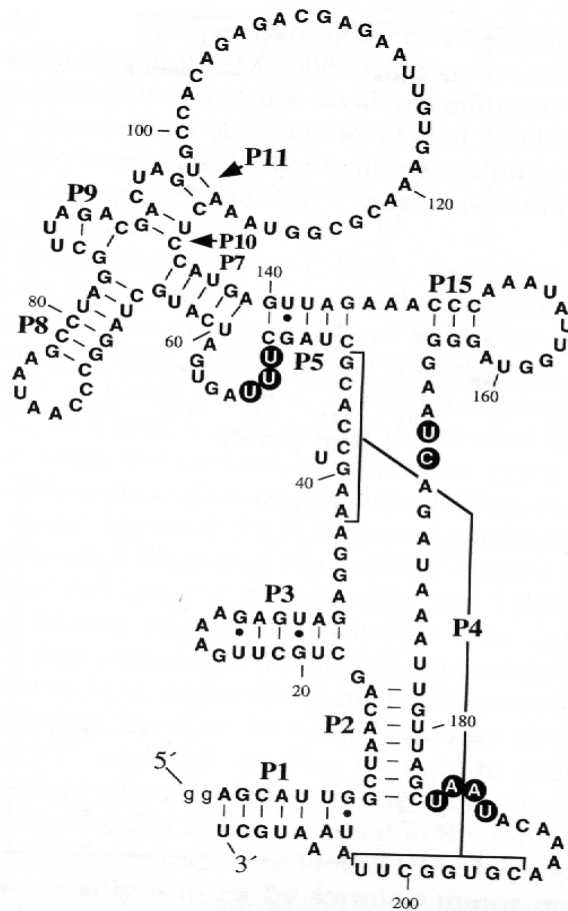


Figure 2. The RNA secondary structure of Micro P, a synthetic but *in vitro* catalytically active RNase P RNA derived from the RNase P from *Mycoplasma fermentans* (a).

Figure 2 References:

a. Siegel, R.W., Banta, A.B., Haas, E.S., Brown, J.W., and N.R. Pace. 1996. *Mycoplasma fermentans* simplifies our view of the catalytic core of ribonuclease P RNA. RNA 2:452-462.

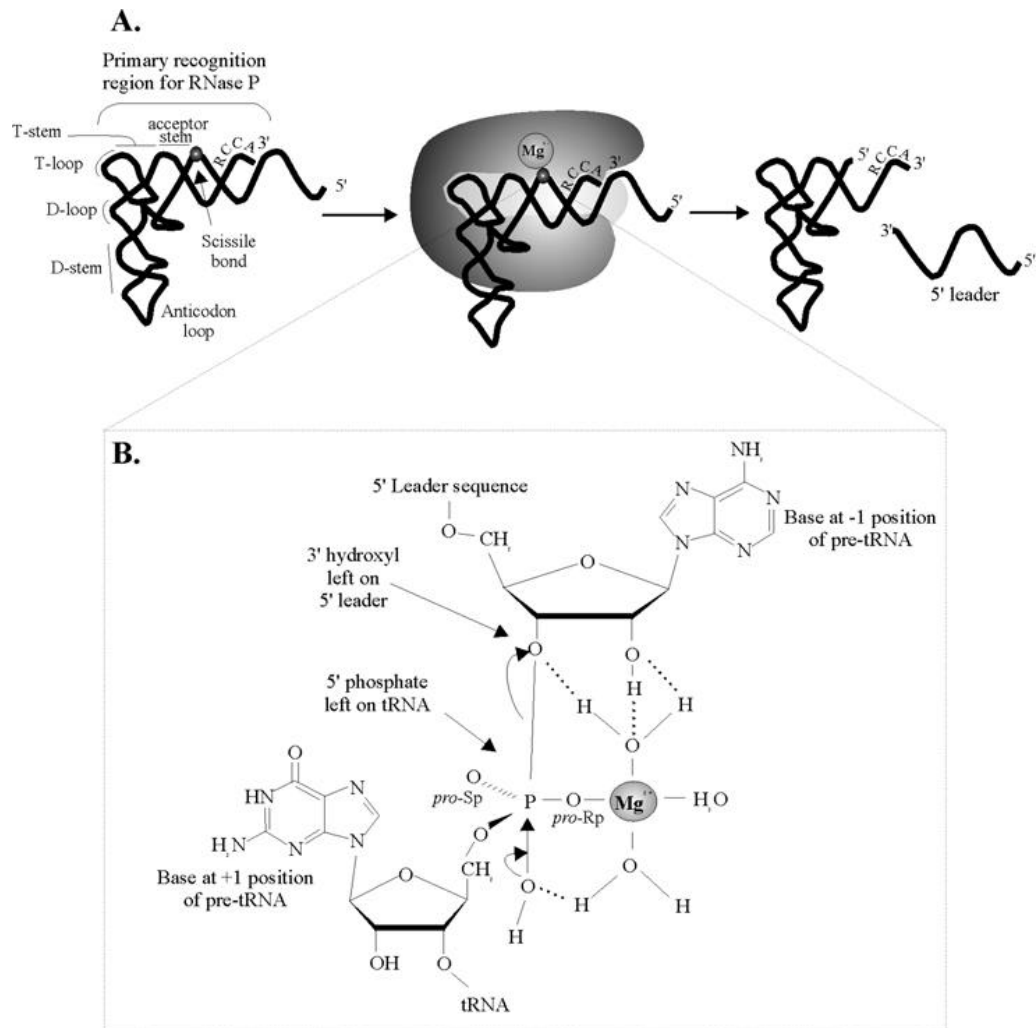


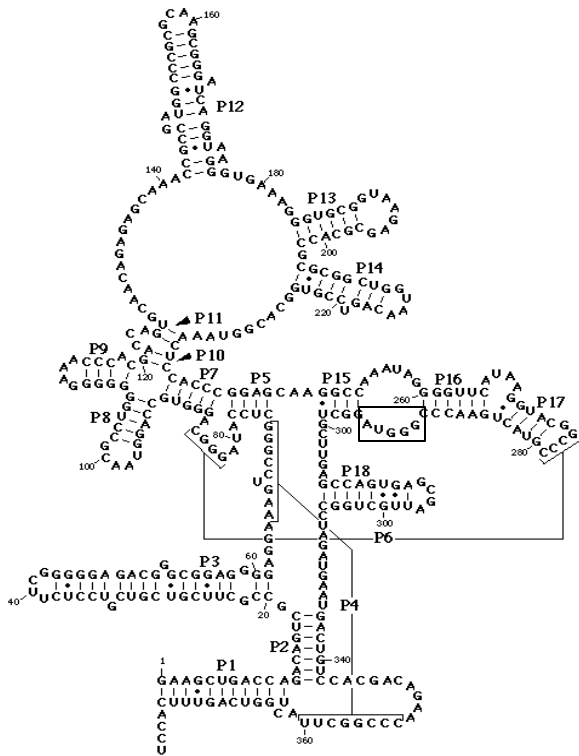
Figure 3. The RNase P reaction. Above is a generalized scheme of RNase P cleavage of pre-cursor tRNA. This reaction occurs in three steps: (1) substrate binding to the holoenzyme via the coaxial stack between acceptor stem and the T loop and ‘NCCA’ binding to the ‘GGU’ sequence of RNase P RNA, (2) cleavage which is diagramed more fully in B utilizing magnesium, and (3) dissociation of products. Part B of this figure diagrams the proposed trigonal pyramide intermediate (a).

Figure 3 References:

a. **Smith, D., and N.R. Pace.** 1993. Multiple magnesium ions in the ribonuclease P reaction mechanism. *Biochemistry* 32:5273-5281.

The Type A Bacterial RNase P RNA

Example: *Escherichia coli*



The Type B Bacterial RNase P RNA

Example: *Bacillus subtilis*

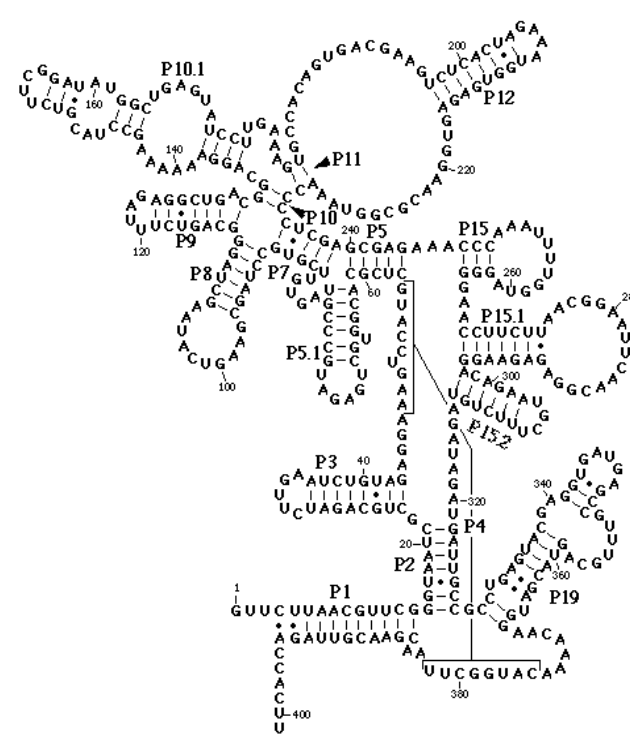
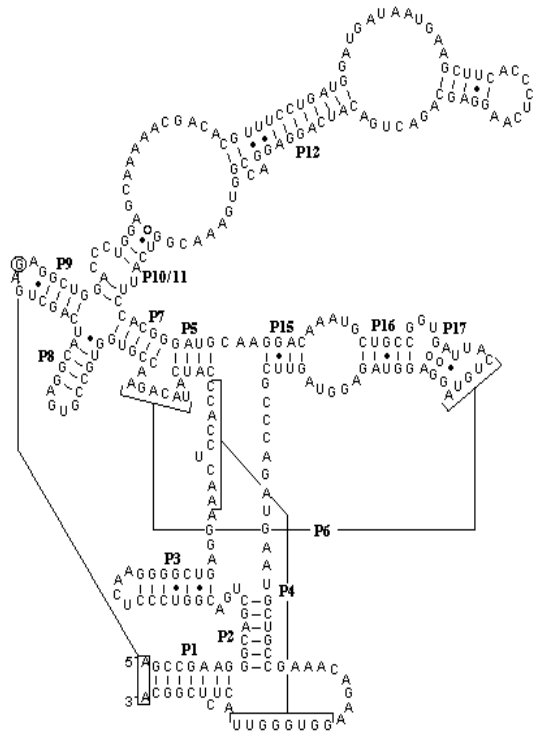


Figure 4. The *E. coli* RNase P RNA secondary structure representing the Type A structures (a) and *B. subtilis* RNase P RNA secondary structure representing the Type B structures (b).

Figure 4 References:

- a. Haas, E.S., A. B. Banta, J. K. Harris, N. R. Pace, and J. W. Brown. 1996. Structure and evolution of ribonuclease P RNA in Gram-positive Bacteria. *Nucleic Acids Res.* 24:4775-4782.
- b. Haas, E.S., Brown, J.W., Pitulle, C., and N.R. Pace. 1994. Further perspective on the catalytic core and secondary structure of ribonuclease P RNA. *Proc. Natl. Acad. Sci.* 91:2527-2531.

Type A Archaeal RNase P RNA
 Example: *Methanothermobacter thermoautotrophicus*



Type B Archaeal RNase P RNA
 Example: *Methanococcus jannaschii*

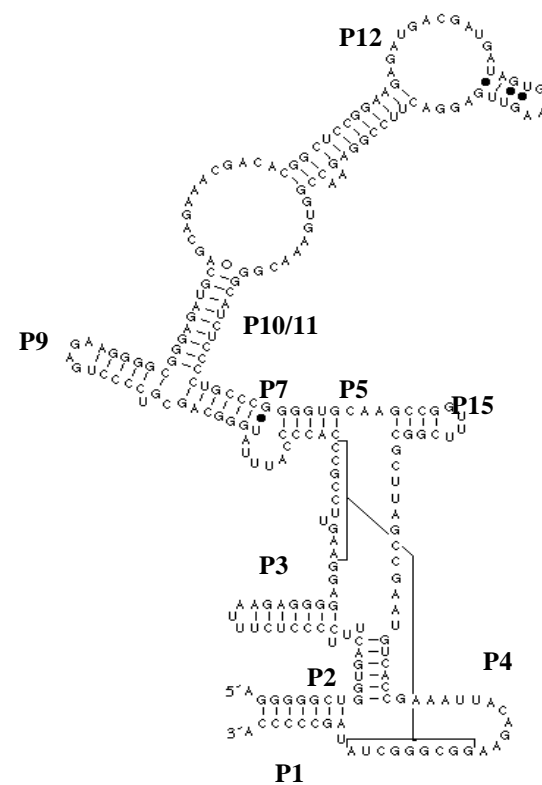
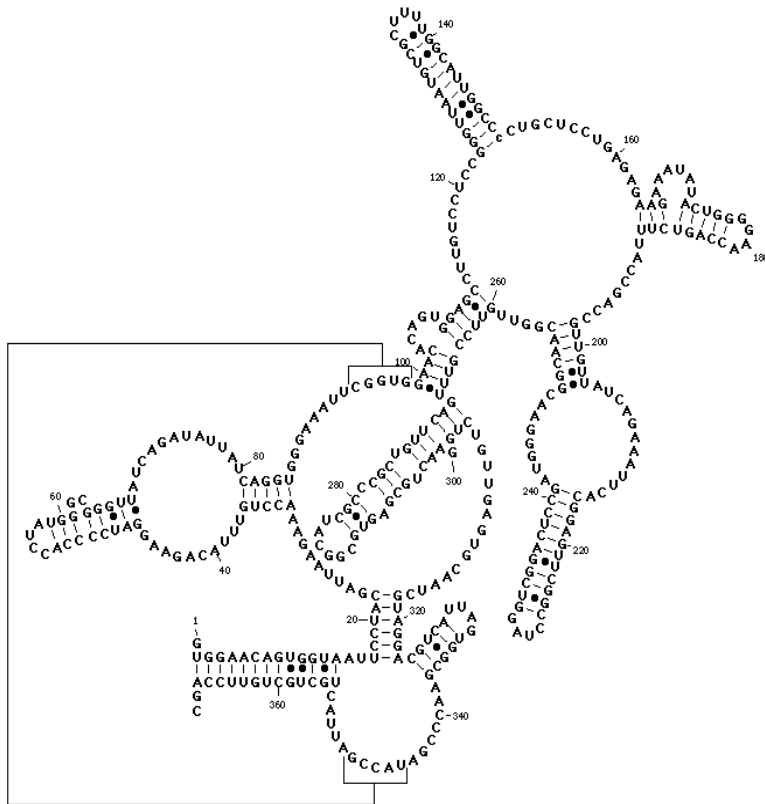


Figure 5. Secondary structures of the RNase P RNAs from *Methanobacterium thermoautotrophicum* delta H strain and of *Methanococcus jannaschii* (a).

Figure 5 References:

a. Harris, J.K., Haas, E.S., Williams, D., Frank, D.N., and J.W. Brown. 2001. New insight into RNase P structure from comparative analysis of the archaeal RNA. RNA 7:220-232.

The RNase P RNA from
Saccharomyces cerevisiae



The RNase P RNA from
Homo sapiens

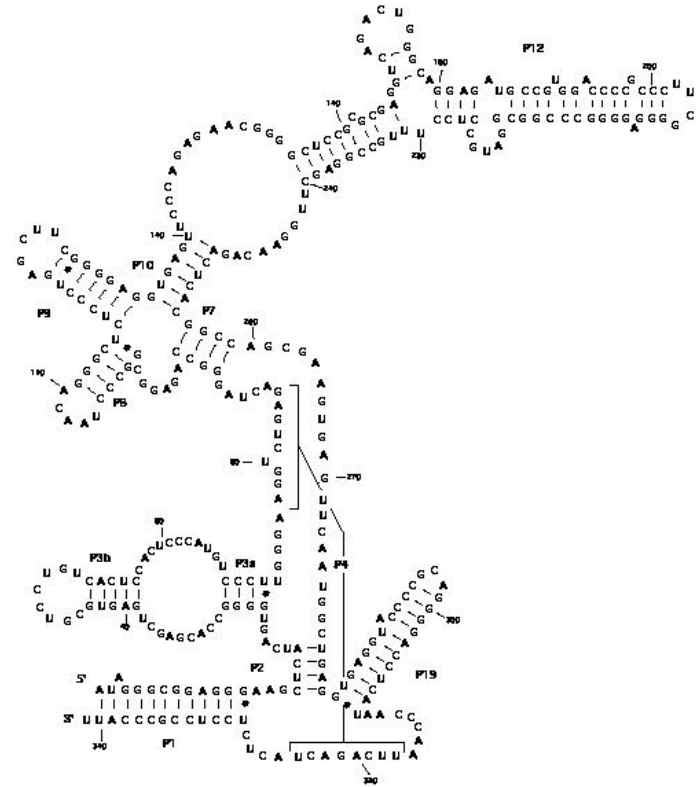


Figure 6. RNase P RNA secondary structures for *Saccharomyces cerevisiae* and *Homo sapiens* (a).

Figure 6 References:

a. Frank, D.N., Adamidi, C., Ehringer, M.A., Pitulle, C., and N.R. Pace. 2000 Phylogenetic-comparative analysis of the eukaryal ribonuclease P RNARNA 6:1895-904.

REFERENCES

1. **Andrews, A. J., Hall, T.A., and J.W. Brown.** 2001. RNase P in methanogenic Archaea. *J. Biol. Chem.* Accepted 6-15-01.
2. **Biswas, R., Ledman, D.W., Fox, R.O., Altman, S., and V. Gopalan.** 2000. Mapping RNA-protein interactions in ribonuclease P from *Escherichia coli* using disulfide-linked EDTA-Fe. *J. Mol. Biol.* 296:19-31.
3. **Brown, J.W..** 1999. The ribonuclease P database. *Nucleic Acids Res.* 27:314
4. **Burgin A.B. and N.R. Pace.** 1990. Mapping the active site of ribonuclease P RNA using a substrate containing a photoaffinity agent. *EMBO J.* 9:4111-4118.
5. **Chamberlain, J.R., Lee, Y., Lane, W.S., and D.R. Engelke.** 1998. Purification and characterization of the nuclear RNase P holoenzyme complex reveals extensive subunit overlap with RNase MRP. *Genes and Dev.* 12:1678-1690.
6. **Chamberlain, J.R., Tranguch, A.J., Pagan-Ramos, E., and D.R. Engelke.** 1996. Eukaryotic nuclear RNase P: structure and functions. *Prog. Nucleic Acid Res. Mol. Biol.* 55:87-119.
7. **Chen, J-L., and N.R. Pace.** 1997. Identification of the universally conserved core of ribonuclease P RNA (letter). *RNA* 3:557-560.
8. **Christian, E.L. and M.E. Harris.** 1999. The track to the pre-tRNA 5' leader in the ribonuclease P ribozyme-substrate complex. *Biochemistry* 38:12623-12638.
9. **Christian, E. L., McPheeters, D.S. and M. E. Harris.** 1998. Identification of individual nucleotides in the bacterial ribonuclease P ribozyme adjacent to the pre-tRNA cleavage site by short-range photo-cross-linking. *Biochemistry* 37:17618-17628.
10. **Cole, K.B., and R.L. Dorit.** 1999. Acquisition of novel catalytic activity by the M1 RNA ribozyme: the cost of molecular adaptation. *J. Mol. Biol.* 292:931-944.
11. **Cole, K.B. and R.L. Dorit.** 2001. Protein cofactor-dependent acquisition of novel catalytic activity by the RNase P ribonucleoprotein of *E. coli*. *J. Mol. Biol.* 307:1181-1193.
12. **Cordier, A. and A. Schon.** 1999. Cyanelle RNase P: RNA structure analysis and holoenzyme properties of an organellar ribonucleoprotein enzyme. *J. Mol. Biol.* 289:9-20.

13. **Crary, S.M., Niranjanakumari, S., and C.A. Fierke.** 1998. The protein component of *Bacillus subtilis* ribonuclease P increases catalytic efficiency by enhancing interactions with the 5' leader sequence of pre-tRNA. *Biochemistry* 37:9409-9416.
14. **Darr, S.C., B. Pace, and N.R. Pace.** 1990. Characterization of ribonuclease P from the archaeobacterium *Sulfolobus solfataricus*. *J. Biol. Chem.* 265:12927-12932.
15. **Darr, S.C., Zito, K., Smith, D., and N.R. Pace.** 1992. Contributions of phylogenetically variable structural elements to the function of the ribozyme ribonuclease P. *Biochemistry* 31:328-333.
16. **Frank, D.N., Ellington, A.E., and N.R. Pace.** 1996. *In vitro* selection of RNase P RNA reveals optimized catalytic activity in a highly conserved structural domain. *RNA* 2:1179-1188.
17. **Frank, D.N. and N.R. Pace.** 1998. Ribonuclease P: Unity and diversity in a tRNA processing ribozyme. *Annu. Rev. Biochem.* 67:153-180.
18. **Guerrier-Takada, C., and S. Altman.** 1993. A physical assay for and a kinetic analysis of the interactions between M1 RNA and tRNA precursor substrates. *Biochemistry* 32:849-857.
19. **Guerrier-Takada, C., K. Gardner, T. Marsh, N. Pace, and S. Altman.** 1983. The RNA moiety of ribonuclease P is the catalytic subunit of the enzyme. *Cell* 35:849-857.
20. **Haas, E. S., D. W. Armbruster, B. M. Vucson, C. J. Daniels, and J.W. Brown.** 1996. Comparative analysis of ribonuclease P RNA structure in Archaea. *Nucleic Acids Res.* 24:1252-1259.
21. **Haas, E.S., A. B. Banta, J. K. Harris, N. R. Pace, and J. W. Brown.** 1996. Structure and evolution of ribonuclease P RNA in Gram-positive Bacteria *Nucleic Acids Res.* 24:4775-4782.
22. **Haas, E.S., Brown, J.W., Pitulle, C., and N.R. Pace.** 1994. Further perspective on the catalytic core and secondary structure of ribonuclease P RNA. *Proc. Natl. Acad. Sci.* 91:2527-2531.
23. **Hardt, W.D., Schlegl, J., Erdmann, V.A., and R.K. Hartmann.** 1993. Role of the D arm and the anticodon arm in tRNA recognition by eubacterial and eukaryotic RNase P enzymes. *Biochemistry* 32:13046-13053.
24. **Harris, J.K., Haas, E.S., Williams, D., Frank, D.N., and J.W. Brown.** 2001. New insight into RNase P structure from comparative analysis of the archaeal RNA. *RNA* 7:220-232.

25. **Harris, M.E., Kazantsev, A.V., Chen, J., and N.R. Pace.** 1997. Analysis of the tertiary structure of the ribonuclease P ribozyme-substrate complex by site specific photoaffinity crosslinking. *RNA* 3:561-576.
26. **Harris, M.E., and N.R. Pace.** 1995. Identification of phosphates involved in catalysis by the ribozyme RNase P RNA. *RNA* 1:210-218.
27. **Heide, C., Busch, S., Feltens, R., and R. K. Hartmann.** 2001. Distinct modes of mature and precursor RNA binding to *Escherichia coli* RNase P RNA revealed by NAIM analyses. *RNA* 7:553-564.
28. **Kirsebom, L.A.** 1995. RNase P--a 'Scarlet Pimpernel'. *Mol. Microbiol.* 17:411-20.
29. **Koonin, E.V., Wolf, Y.I., and L. Aravind.** 2001. Prediction of the archaeal exosome and its connections with the proteasome and the translation and transcription machineries by a comparative-genomic approach. *Genome Res.* 11:240-252.
30. **Kurz, J.C., Niranjankumari, S., and C.A. Fierke.** 1998. Protein component of *Bacillus subtilis* RNase P specifically enhances the affinity for precursor-tRNA^{Asp}. *Biochemistry* 37:2393-2400.
31. **LaGrandeur, T.E., S.C. Darr, E.S. Haas, and N.R. Pace.** 1993. Characterization of the RNase P RNA of *Sulfolobus acidocaldarius*. *J. Bacteriol.* 175:5043-5048.
32. **LaGrandeur, T.E., Hüttenhofer, A., Noller, H.F., and N.R. Pace.** 1994. Phylogenetic comparative chemical footprint analysis of the interaction between ribonuclease P RNA and tRNA. *EMBO J.* 13:3945-3952.
33. **Lawrence, N., Wesolowski, D., Gold, H., Bartkiewicz, M., Guerrier-Takada, C., McClain, W.H., and S. Altman.** 1987. Characteristics of ribonuclease P from various organisms. *Cold Spring Harbor Symp. Quant. Biol.* 52:233-238.
34. **Li, Y. and S. Altman.** 2000. A subunit of human nuclear RNase P has ATPase activity. *Proc. Natl. Acad. Sci.* 98:441-444.
35. **Loria, A. and T. Pan.** 1998. Recognition of the 5' leader and acceptor stem of pre-tRNA substrate by the ribozyme from *Bacillus subtilis* RNase P. *Biochemistry* 37:10126-10133.
36. **Loria, A. and T. Pan.** 2000. The 3' substrate determinates for the catalytic efficiency of the *Bacillus subtilis* RNase P holoenzyme suggest autolytic processing of the RNase P RNA in vivo. *RNA* 6:1413-1422.

37. **Loria, A. and T. Pan.** 2001. Modular construction for function of a ribonucleoprotein enzyme: the catalytic domain of *Bacillus subtilis* RNase P with *B. subtilis* RNase P protein. *Nucleic Acids Res.* 29:1892-1897.
38. **Morse, D.P. and F.J. Schmidt.** Suppression of loss-of-function mutations in *Escherichia coli* ribonuclease P RNA (M1 RNA) by a specific base-pair disruption. 1993. *J. Mol. Biol.* 230:11-4
39. **Niranjanakumari, S., Stams, T., Crary, S.M., D.W. Christianson, and C.A. Fierke.** 1998. Protein component of the ribozyme ribonuclease P alters substrate recognition by directly contacting precursor tRNA. *Proc. Natl. Acad. Sci.* 95:15212-15217.
40. **Nolan, J.M., D.H. Burke, and N.R. Pace.** 1993. Circularly permuted tRNAs as specific photoaffinity probes of ribonuclease P RNA structure. *Science* 261:762-765.
41. **Oh, B.K. and N.R. Pace.** 1994. Interaction of the 3'-end of tRNA with ribonuclease P RNA. *Nucleic. Acids. Res.* 22:4087-94.
42. **Pace, N.R. and J.W. Brown.** 1995. Evolutionary perspective on the structure and function of ribonuclease P, a ribozyme. *J. Bacteriology* 177:1919-28
43. **Pace, N.R., and D. Smith.** 1990. Ribonuclease P: function and variation. *J. Biol. Chem.* 265:3587-3590.
44. **Pannucci, J.A., Haas, E.S., Hall, T.A., Harris, J.K., and J.W. Brown.** 1999. RNase P RNAs from some Archaea are catalytically active. *Proc. Natl. Acad. Sci.* 96:7803-7808.
45. **Peck-Miller, K.A., and S. Altman.** 1991. Kinetics of the processing of the precursor to 4.5 S RNA, a naturally occurring substrate for RNase P from *Escherichia coli*. *J. Mol. Biol.* 221:1-5.
46. **Pomeranz Krummel, D.A. and S. Altman.** 1999. Multiple binding modes of substrate to the catalytic RNA subunit of RNase P from *Escherichia coli*. *RNA* 5:1021-1033.
47. **Reich, C., Olsen, G.J., Pace, B., and N.R. Pace.** 1988. Role of the protein moiety of ribonuclease P a ribonucleoprotein enzyme. *Science* 239:178-181.
48. **Rossmannith, W., and R.M. Karwan.** 1998. Characterization of human mitochondrial RNase P: novel aspects in tRNA processing. *Biochem. Biophys. Res. Commun.* 247: 234-241.
49. **Schedl, P., Primakoff, P., and J. Roberts.** 1975. Processing of *Escherichia coli* tRNA processors. *Brookhaven Symp Biol* Jul;(26):53-76.

50. **Schon, A.** 1999. RNase P: the diversity of a ubiquitous RNA processing enzyme. *FEMS Microbiology Reviews* 23:391-406.
51. **Siegel, R.W., Banta, A.B., Haas, E.S., Brown, J.W., and N.R. Pace.** 1996. *Mycoplasma fermentans* simplifies our view of the catalytic core of ribonuclease P RNA. *RNA* 2:452-462.
52. **Siew, D., Zahler, N.H., Cassano, A.G., Strobel, S.A., and M. E. Harris.** 1999. Identification of adenosine functional groups involved in substrate binding by the ribonuclease P ribozyme. *Biochemistry* 38: 1873-1883.
53. **Smith, D., Burgin, A.B., Haas, E.S., and N.R. Pace.** 1992. Influence of metal ions on the ribonuclease P reaction. *J. Biol. Chem.* 267:2429-2436.
54. **Smith, D., and N.R. Pace.** 1993. Multiple magnesium ions in the ribonuclease P reaction mechanism. *Biochemistry* 32:5273-5281.
55. **Stams, T., Niranjanakumari, S., Fierke, C. A., and D.W. Christianson.** 1998. Ribonuclease P protein structure: evolutionary origins in the translational apparatus. *Science* 280:752-755.
56. **Stark, B.C., Kole, R., Bowman, E.J., and S. Altman.** 1978. Ribonuclease P: an enzyme with an essential RNA component. *Proc. Natl. Acad. Sci.* 75:3717-3721.
57. **Thomas, B.C., Xinqiang, L., and P. Gegenheimer.** 2000. Chloroplast ribonuclease P does not utilize the ribozyme-type pre-tRNA cleavage mechanism. *RNA* 6:545-553.
58. **Vioque, A., Arnez, J., and S. Altman.** 1988. Protein-RNA interactions in the RNase P holoenzyme from *Escherichia coli*. *J. Mol. Biol.* 202: 835-48.
59. **Wolin, S.L., and A.G. Matera.** 1999. The trials and travels of tRNA. *Genes & Dev.* 13:1-10.
60. **Xiao, S., Houser-Scott, F., and D.R. Engelke.** 2001. Eukaryotic ribonuclease P: increased complexity to cope with the nuclear pre-tRNA pathway. *J. Cell. Phys.* 187:11-21.

CHAPTER ONE: IDENTIFICATION OF SUBSTRATE-HOLOENZYME

INTERACTIONS IN *METHANOCOCCUS JANNASCHII* RNASE P

ABSTRACT

RNase P is the enzyme responsible for the 5' end maturation of all pre-cursor tRNAs. In Bacteria the RNA alone is capable of cleaving substrate *in vitro*. This protein free activity is not seen in the RNase P RNAs characterized from Eukaryotes and the few archaeal RNase P RNAs that can perform the cleavage reaction must do so at very high ionic strength. No Type M RNAs from Archaeal RNase Ps are capable of the *in vitro* reaction without their protein co-factors. Because the holoenzymes containing type M RNAs are functional *in vitro* and *in vivo* they must have all the components necessary for substrate interaction present. In Bacteria, regions in the RNA subunit where precursor tRNA interacts have been identified (P8, L15/P16/P17, and the catalytic center surrounding P4). Elements P8 and L15/P16/P17 are missing in the type M RNAs and no extra secondary structures are present that might replace their function. The holoenzyme for *M. jannaschii*, containing a type M RNA, has been purified and appears to contain more than one protein cofactor. It is possible that one or more of these proteins contains the substrate binding domain of this enzyme compensating for the lack of P8 and L15. A method is described herein by which RNase P holoenzyme-substrate T loop interactions can be identified using circularly permuted transfer RNAs. The 5' end of these substrates is located in the T loop where guanosine monophosphorothioate can be incorporated during transcription, and a photoagent attached after purification. Upon excitation with ultraviolet light the photoagent should covalently cross-link to close-by chemical groups.

We predict that these substrates will cross-link to one or more protein subunits within the *M. jannaschii* holoenzyme.

INTRODUCTION

The RNase P RNAs from Archaea vary in their ability to cleave premature tRNA (pre-tRNA) *in vitro* in the absence of protein and those RNAs that can cleave substrate only do so with high salt concentration (13). This ability to cleave substrate suggests that the active RNAs have the secondary structures necessary for activity but fail to form the required tertiary structure without protein. All RNase P RNAs from the Archaea resemble their bacterial counterparts in secondary structure, and they have been divided into two distinct groups based on their differences and similarities (6). Type A RNAs (the ancestral type) resemble the secondary structure of bacterial RNA most closely although they lack helices P13/14 and P18 (Figure 1). Type A RNAs are found in both branches of the Archaea, the Crenarchaea and the Euryarchaea. Of the Euryarchaea, RNase P RNAs from methanobacteria, extreme halophiles, and thermococci have ribozyme activity (13). Type M RNAs resemble type A RNAs except they lack 3 major components: P6, P8, and element L15/P16P/17 (Figure 1). In the bacterial ribozyme the helix P8 as well as the helix and loop structures distal to P15 have been shown through cross-linking and mutation experiments to interact with pre-tRNA substrates, P8 with the T loop and J15/16 with the 3'CCA tail (4,12). Also, the tertiary interactions forming P6 by L17 and J5/7 are also absent in type M RNAs. The type M RNAs do not contain extra secondary structure that could form remunerative interactions. The absence of these important substrate binding domains and tertiary interactions is presumably efficient enough to render the RNAs inactive without their associated proteins.

These inactive RNase P RNAs are able to cleave pre-tRNA *in vivo* and purified extracts of RNase Ps with type M RNAs are active *in vitro*. The presence of the protein

subunits accompanying the RNA correlates with activity showing their importance in the holoenzyme. Where as bacterial RNase Ps have a single RNA subunit accompanied by a single protein cofactor, the holoenzymes isolated from members of the Archaea seem to have a varying amount of associated protein (1,3,5,10). The buoyant densities of two archaeal RNase Ps, those of *Sulfolobus acidocaldarius* and *Haloferax volcanii*, support the notion that archaeal RNase Ps vary in protein content between members. *S acidocaldarius* RNase P has a buoyant density in Cs₂SO₄ of 1.27g/ml which indicates a high protein content whereas *H. volcanii* RNase P has a buoyant density of 1.61g/ml, close to that of single-stranded RNA (1.65g/ml) (3,10,11). These holoenzymes also vary in their sensitivity to nuclease treatment, *H. volcanii* is sensitive to micrococcal nuclease but the RNase P from *S acidaldarius* is insensitive to the same treatment (3,9). The RNA component of *S acidaldarius* RNase P has been characterized and is probably shielded from nucleases by its protein subunits and/or the cesium used in purifying them (9).

RNase Ps isolated from the methanogenic Archaea has recently provided new information about archaeal RNase Ps and reveals that RNase Ps among the Archaea are more similar than previously thought (1). The RNase P of *Methanothermobacter thermoautotrophicus* (formally know as *Methanobacterium thermoautotrophicum* ΔH) and the RNase P from *Methanococcus jannaschii* have buoyant densities in the median between that of bulk protein and single-stranded RNA, 1.42g/ml and 1.39g/ml respectively (1). These two enzymes have a single bacteria-like RNA subunit and as many as nine associated protein subunits. Four RNase P protein encoding open reading frames in the genomes of both methanogens have been identified by their similarity to *Saccharomyces cerevisiae* nuclear RNase P proteins (Pop4p, Pop5p, Rpp1p and Rpr2p).

Homologues to these proteins have also been found in the genomes other Archaea as well as in nuclear RNase P of HeLa cells (Hall and Brown, submitted). The correlation between those proteins in their positions within the genome also supports their potential role in pre-tRNA processing (8). Immunoprecipitation and yeast two-hybrid data support that the four protein homologues in *M. thermoautotrophicus* are in fact RNase P subunits (Hall and Brown, submitted). In eukaryotic cells, RNase Ps having multiple protein subunits are rationalized by the need for other functions in the increased complexity and compartmentalization of the cell. However, it has also been hypothesized that the protein subunits of the type M RNase P RNAs may have acquired some of the functions previously held by the RNA in order to compensate for the loss of substrate interacting secondary structures (13).

Here we investigate the possibility of protein-substrate interactions in the *M. jannaschii* holoenzyme through the use of circularly permuted pre-tRNAs (cptRNAs) with a modified 5' end involving the incorporation of guanosine monophosphorothiate (GMPS) used to attached a photoagent. These substrates, shown in Figure 2, have been used previously in studying substrate interaction with the *Eschericia coli* ribozyme and are cleaved by RNase P *in vitro*, though with lower catalytic efficiency by *E. coli* RNase P (12). The cptRNAs contain a relocated 5' end in the T arm where a (positions 53 or 64) GMPS is incorporated during *in vitro* transcription. The GMPS is then coupled to a photoagent, azidophenacyl bromide, via a nucleophilic displacement of the bromine group (2). Upon excitation with ultraviolet light the azidophenacyl converts to a nitrene which inserts itself into neighboring bonds (2). The nitrene-phenacyl is relatively small, approximately 9 Å in length (2), and forms covalent interactions with bases within short

range of the T loop of the cptRNA substrate. UV cross-linking has been successfully used to explore RNA secondary structure and enzyme-substrate interactions (7, 13).

In *E. coli* RNase P RNA, cptRNAs with a modification at position 53 cross-link to positions 110-114 of the P9 loop (12). Since *M. jannaschii* RNase P has helix P9, a cross-link should occur with this substrate. Substrate with the photoagents at position 64 crosslinks to positions 98-102 in the P8 helix of *E. coli* RNase P RNA (12). *M. jannaschii* is a type M RNA and therefore lacks the P8 helix and loop which cross-link to cptRNA substrates in *E. coli* RNase RNA. We predict that upon excitation with UV light the cptRNAs will become covalently linked to one of several protein subunits of *M. jannaschii* RNase P.

MATERIALS AND METHODS

***In vitro* transcription reactions**

Unlabelled RNase P RNAs were transcribed using recombinant T7 RNA polymerase in a run-off transcription reaction using 10mM DTT, Promega T7 transcription buffer, 0.5mM nucleotide triphosphates, approximately 0.5µg of template, and 1µl of recombinant T7 polymerase. Reactions were incubated for 4 hours at 37°C. Transcription products were run on a 4% polyacrylamide gel and viewed by UV shadowing on PEI plates. RNAs correlating to the expected size were excised and passively eluted into 10mM Tris pH 8, 1mM EDTA and 0.1% SDS buffer, phenol/chloroform extracted, ethanol precipitated, and quantitated by UV spectrophotometry.

Pre-tRNA substrates were transcribed using recombinant T7 polymerase (Promega) in 20µl of 10mM DTT, 0.5mM AUGC mix, 5µl of radioactive UTP, and 4µl

of 5X transcription buffer. Reactions ran for 2 hours at 37°C, and products were resolved on a 6% polyacrylamide gel.

³²P labeled cptRNA substrates were transcribed using a Mega Short Script kit by Ambion. The only alteration to the kit protocol was the addition of 10mM GMPS in the reaction mixture when required. Reaction products were resolved on a 6% polyacrylamide gel and visualized by autoradiography. Products of the correct size were excised and purified as described above. Circularly permuted tRNAs were quantitated by scintillation spectroscopy.

RNase P activity assays

RNase P assay reactions contained 3µl of enzyme (either RNase P RNA alone or holoenzyme), RNase P Assay buffer (100mM ammonium acetate, 25mM MgCl₂, 0.05% nonidet P-40, and 50mM tris), 6000cpm of ³²P labelled substrate (pre-tRNA^{asp}) and water up to 10µl. This reaction mixture was incubated for 15 minutes at 37°C. Reaction products were resolved on a 12% polyacrylamide urea gel. Bands were quantified by phosphorimager, and the percent cleavage for each reaction was calculated.

UV cross-linking

M. jannaschii RNase P extracts and cptRNAs used in ultraviolet cross-linking reactions were obtained by standard purification methods previously described in Andrews, et. al. 2001. Cross-linking reactions were performed using a 1:50 ratio of substrate to enzyme, incubated at 37°C for 5 minutes to allow for binding, and exposed to UV light for 45 minutes. Such conditions have been used previously without resulting in non-specific cross-linking (2,5). Control experiments were performed using either *M.*

jannaschii or *E. coli* RNase P RNA produced by *in vitro* T7 transcription in place of *M. jannaschii* RNase P holoenzyme, or no enzyme at all.

Photoagent-substrate coupling

Full length cptRNA transcripts were gel purified as stated above and the dried pellet was dissolved in 33 mM sodium bicarbonate, pH 9.0. p-azidophenacyl bromide in methanol was added to 12 mM. The mixture was incubated at room temperature for 1 hour. The samples were phenol extracted to remove any excess photoagent and the substrates were re-suspended in 20ul of water. All procedures involving azidophenacyl bromide were performed in the dark.

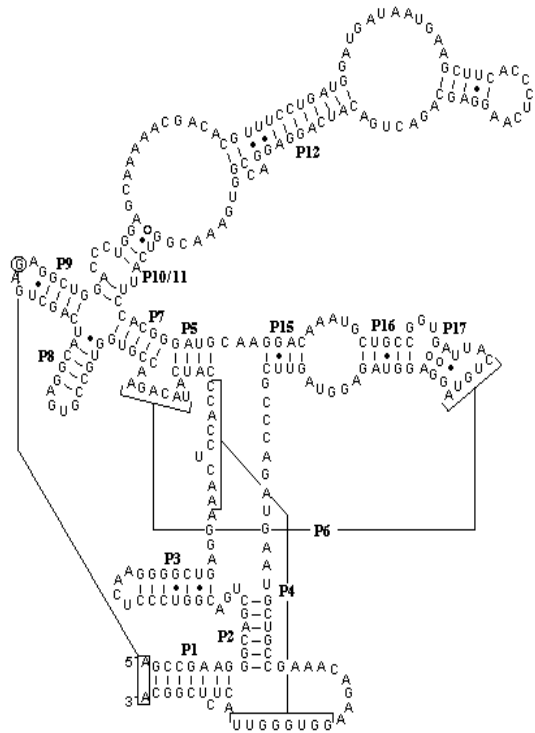
RESULTS AND DISCUSSION

In vitro transcription reactions performed using T7 RNA polymerase were successful for the production of *B. subtilis* pre-tRNA^{Asp} substrate but were not successful in producing sufficient amounts of GMPS incorporated cptRNA transcripts for cross-linking reactions. Despite the low concentrations of gel purified cptRNAs produced, these substrates were used in azidophenacyl bromide coupling reactions and subsequently in a UV-cross-linking experiment (Figure 4). *M. jannaschii* RNase P extracts verified to have RNase P activity by their ability to cleave synthetic pre-tRNA^{Asp} substrate did not UV-crosslink to the cptRNAs. However, the *E. coli* RNase P RNA positive control did not crosslink to the cptRNAs either indicating that something was wrong with either the controls or with the cptRNAs. The *E.coli* RNA was tested for its ability to cleave pre-tRNA^{Asp} substrate and was determined to be active. This implicates that the cptRNAs were not functioning as cross-linking substrates under the excitement of UV light.

Three aspects of this experiment could be responsible for the failure of substrate photoreactivity in the substrate. (1) It is possible that the concentration of cptRNA was too low in the reaction. During the purification of photo-reactive cptRNAs, they are phenol extracted twice, first to remove any acrylamide or residual transcription contaminants in them, and second to remove any unreacted azidophenacyl bromide after the nucleophilic coupling reaction. Both of these extractions risk the loss of substrate and thus lower the amount of final substrate recovered. (2) GMPS may not have been incorporated into the 5' end of the cptRNAs. Since T7 transcription requires triphosphates for elongation but only a monophosphate for initiation, GMPS will only be incorporated at the 5' end of the transcript. However, the ratio of GMPS to GTP must be 10:1 in a 20ul transcription reaction and does not always produce high incorporation. (3) Finally, the azidophenacyl bromide group may not have attached to the 5' GMPS. Azidophenacyl bromide is soluble in methanol, but must be mixed with calcium carbonate, pH 9, in order to become reactive to the thioate group on GMPS (2). Two ways of performing this reaction have been described in detail. One method features the addition of a prescribed amount of azidophenacyl bromide (in methanol) to substrate already resuspended in CaCO₃, and the other uses a mixture of these two reagents to directly re-suspend the substrate. Both of these methods were performed and precipitation of the azidophenacyl bromide occurred upon addition of methanol to the solution. The procedures for coupling azidophenacyl bromide to a 5'GMPS labeled RNA have been described several times in the literature and no mention of its precipitation has been mentioned (2,7,12,14). The lack of dissolved photoagent could have prevented successful cross-linking. The inconclusive results from these experiments do not rule out the possible protein-substrate interaction proposed. It

remains to be seen what subunits of the RNase P holoenzyme from *M. jannaschii* interact with pre-tRNA.

Type A Archaeal RNase P RNA
 Example: *Methanothermobacter thermoautotrophicus*



Type M Archaeal RNase P RNA
 Example: *Methanococcus jannaschii*

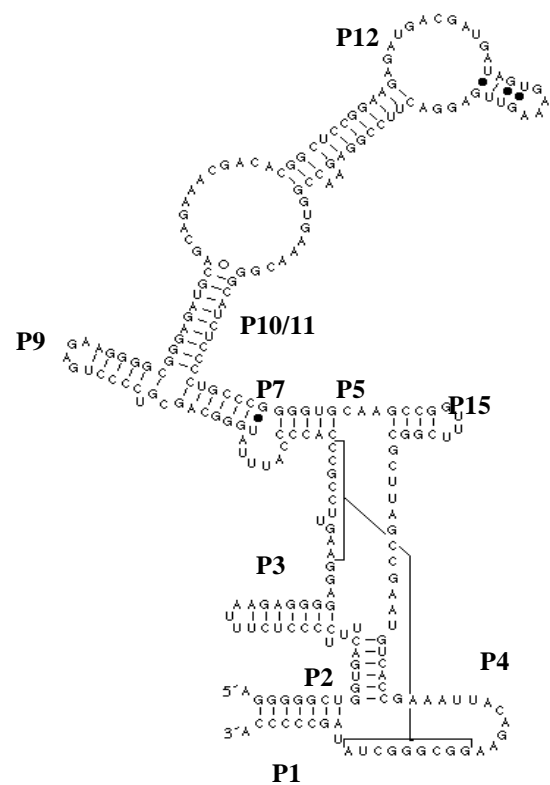


Figure 1. Secondary structures of the RNase P RNAs from *Methanothermobacter thermoautotrophicus* strain and *Methanococcus jannaschii* (a).

Figure 5 References:

- a. **Harris, J.K., Haas, E.S., Williams, D., Frank, D.N., and J.W. Brown.** 2001. New insight into RNase P structure from comparative analysis of the archaeal RNA. *RNA* 7:220-232.

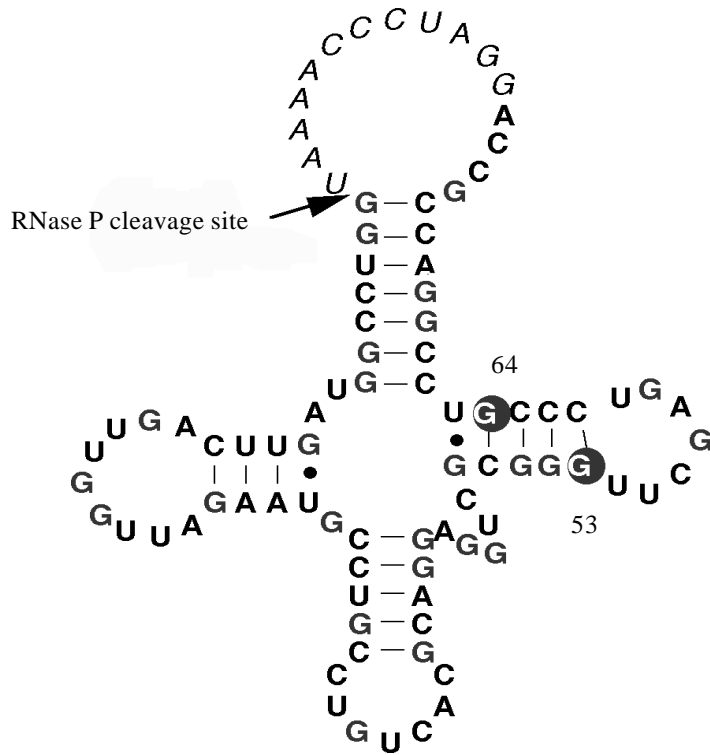


Figure 2. Circularly permuted pre-tRNA. The RNase P cleavage site is indicated by an arrow and the linker sequences are italicized. Positions where GMPS are incorporated are circled and numbered.

Figure 2 References:

a. **Nolan, J.M., D.H. Burke, and N.R. Pace.** 1993. Circularly permuted tRNAs as specific photoaffinity probes of ribonuclease P RNA structure. *Science* 261:762-765.



Figure 3. UV crosslinking of cptRNA to *M. jannaschii* RNase P. No crosslinking was detected even for the control reactions. Unreacted substrate is indicated by an arrow.

REFERENCES

1. **Andrews, A. J., Hall, T.A., and J.W. Brown.** 2001. RNase P in methanogenic Archaea. *J. Biol. Chem.* Accepted 6-15-01.
2. **Burgin A.B. and N.R. Pace.** 1990. Mapping the active site of ribonuclease P RNA using a substrate containing a photoaffinity agent. *EMBO J.* 9:4111-4118.
3. **Darr, S.C., B. Pace, and N.R. Pace.** 1990. Characterization of ribonuclease P from the archaeobacterium *Sulfolobus solfataricus*. *J. Biol. Chem.* 265:12927-12932.
4. **Frank, D.N. and N.R. Pace.** 1998. Ribonuclease P: unity and diversity in a tRNA processing ribozyme. *Annu. Rev. Biochem.* 67:153-180.
5. **Guerrier-Takada, C., K. Gardner, T. Marsh, N. Pace, and S. Altman.** 1983. The RNA moiety of ribonuclease P is the catalytic subunit of the enzyme. *Cell* 35:849-857.
6. **Harris, J.K., Haas, E.S., Williams, D., Frank, D.N., and J.W. Brown.** 2001. New insight into RNase P structure from comparative analysis of the archaeal RNA. *RNA* 7:220-232.
7. **Harris, M.E., and E.L. Christian.** 1999. Use of circular permutation and end modification to position photoaffinity probes for analysis of RNA structure. *Methods* 18:51-59.
8. **Koonin E.V., Wolf, Y.I. and L. Aravind.** 2001. Prediction of the archaeal exosome and its connections with the proteasome and the translation and transcription machineries by a comparative-genomic approach. *Genome Res.* 11:240-252.
9. **LaGrandeur, T.E., Darr, S.C., Haas, E.S., and N.R. Pace.** 1993. Characterization of the RNase P RNA of *Sulfolobus acidocaldarius*. *J. Bacteriol.* 175:5043-5048.
10. **Lawrence, N., Wesolowski, D., Gold, H., Bartkiewicz, M., Guerrier-Takada, C., McClain, W.H., and S. Altman.** 1987. Characteristics of ribonuclease P from various organisms. *Cold Spring Harbor Symp. Quant. Biol.* 52:233-238.
11. **Nieuwlandt, D.T., Haas, E.S., and C.J. Daniels.** 1991. The RNA component of RNase P from the archaeobacterium of *Haloferax volcanii*. *J. Biol. Chem.* 266:5689-5695.
12. **Nolan, J.M., D.H. Burke, and N.R. Pace.** 1993. Circularly permuted tRNAs as specific photoaffinity probes of ribonuclease P RNA structure. *Science* 261:762-765.
13. **Pannucci, J.A., Haas, E.S., Hall, T.A., Harris, J.K., and J.W. Brown.** 1999. RNase P RNAs from some Archaea are catalytically active. *Proc. Natl. Acad. Sci.* 96:7803-7808.

14. **Thomas, B.C., Kavantsev, A.V., Chen, J-L, and N.R. Pace.** 2000. Photoaffinity cross-linking and RNA structural analysis. *Methods Enzymol.* 318:136-147.

CHAPTER TWO: PURIFICATION AND CHARACTERIZATION OF RNASE P PROTEIN SUBUNITS FROM *METHANOCOCCUS JANNASCHII*

ABSTRACT

All precursor transfer RNAs must undergo 5' end processing to become mature tRNAs. The endoribonuclease responsible for this is RNase P, a ubiquitous and essential enzyme which removes the 5' leader sequence from all pre-tRNAs. RNase P of Bacteria has been extensively characterized, and contains a single 14kDa protein along with a ~300 to 400 nucleotide RNA subunit. In the case of bacterial and some archaeal RNase Ps, the RNA subunit alone can cleave pre-tRNA substrate *in vitro* without its protein cofactor. Although the archaeal RNase P RNA resembles the bacterial RNA, it has multiple protein subunits associated with it. Previously only two archaeal RNase Ps had been purified and characterized, indicating by buoyant density in Cs₂S₀₄ and nuclease sensitivity that the archaeal RNase Ps differ significantly. *Sulfolobus acidocaldarius* RNase P retains its activity after nuclease treatment and has a buoyant density close to that of bulk protein (1.27g/ml). On the other hand, *Haloferax volcanii* RNase P is highly sensitive to nuclease and has a buoyant density of 1.65g/ml in Cs₂S₀₄, close to that of single stranded RNA. More recent data from the methanogenic Archaea, *Methanothermobacter thermoautotrophicus* and *Methanococcus jannaschii*, reveals that archaeal RNase Ps may have more in common with each other than the data from *S. acidocaldarius* and *H. volcanii* suggested. Although the RNA subunits of archaeal RNase Ps have been identified, little is known about the protein subunits of these enzymes. In order to learn more about these diverse ribonucleases, the RNase P was purified from *M. jannaschii* and the protein subunits co-purifying with activity were analyzed by MALDI-

TOF mass spectrometry. Here we established the presence of MJ1139 and MJ0464, two predicted RNase P proteins, and several other conserved hypothetical proteins in purified RNase P extracts. The 30S ribosomal proteins S6E and S8E and a nicotinamide-nucleotide adenylyltransferase were also identified as co-purifying with *M. jannaschii* RNase P.

INTRODUCTION

RNase P is the enzyme responsible for 5' maturation of precursor tRNAs in all living organisms (5). RNase P has been extensively characterized in Bacteria and moderately explored in the Eukarya (4). In the Archaea, little is known about the RNase P holoenzymes, and until recently, RNase P holoenzymes have been partially characterized from only two of the Archaea, the Crenarchaea *Sulfolobus acidocaldarius* and the Euryarchaea *Haloferax volcanii* (9). The RNase P from *H. volcanii* has a buoyant density in Cs_2SO_4 of 1.61g/ml, close to that of RNA alone, and is highly sensitive to nuclease treatment, whereas the holoenzyme from *S. acidocaldarius* has a buoyant density of 1.27g/ml indicating that it is largely made of protein and is insensitive to nuclease treatment (3,11). The biochemical characteristics of the RNase Ps from these two organisms contradict each other leading to the idea that archaeal RNase Ps may have little in common with each other.

Recently, the biochemical characteristics of two methanogenic Archaea, *Methanococcus jannaschii* and *Methanothermobacter thermoautotrophicus*, have suggested that archaeal RNase Ps may have more in common than previously thought. The RNase Ps from *M. jannaschii* and *M. thermoautotrophicus* have buoyant densities in the median between that of bulk protein (1.39g/ml) and single-stranded RNA (1.42g/ml) (1). The RNAs of these enzymes have been known for some time, and characteristics of their activity and their secondary structures determined, however almost nothing is known of the proteins that associate with them. The RNAs found in archaeal RNase Ps resemble those found Bacteria, but the buoyant densities of isolated holoenzymes indicate significant protein content as seen in eukaryotic RNase Ps. No open reading frames have

been identified in archaeal genomes that would encode a protein homologous to bacterial RNase P proteins (13).

The RNase P holoenzyme of *Saccharomyces cerevisiae* was purified to homogeneity and was shown to contain nine proteins whose identities were determined via mass spectrometry (2). Four *M. thermoautotrophicus* proteins (MTH11, MTH687, MTH688, MTH1618) have been identified as possible RNase P subunits by their apparent homology to four of the nine *S. cerevisiae* proteins (Pop4p, Pop5p, Rpp1p, Rpr2p) which co-purify with RNase P (Hall and Brown, submitted). Antibodies raised against these four potential *M. thermoautotrophicus* RNase P proteins were able to immunoprecipitate RNase P activity from *M. thermoautotrophicus* cell extracts (Hall and Brown, submitted). Western blot analysis using those same antibodies confirmed the co-purification of all four proteins in RNase P purified from cell extracts (Hall and Brown, submitted).

Those four *M. thermoautotrophicus* RNase P proteins have homologues in other Archaea. In *M. jannaschii* these homologues are MJ0464, MJ0494, MJ0962, and MJ1139 (corresponding respectively to MTH11, MTH687, MTH1618, and MTH688). Two of these proteins, MJ1139 and MJ0494, have previously been predicted to be RNase P proteins based on their position in a super-operon containing ribosomal proteins and other processing proteins (8). Here we confirm the presence of MJ1139 and MJ0464 in highly purified RNase P extracted from *M. jannaschii* along with several conserved and non-conserved hypothetical proteins using MALDI-TOF mass spectrometry.

MATERIALS AND METHODS

Glycerol gradients

“Fraction #44” of Q-sepharose purified *M. jannaschii* RNase P was applied to four 5ml glycerol gradients. Details of the origin of “fraction #44” can be found in Andrews et. al. 2001. These gradients generated from 31 fractions ranging from 10% to 40% glycerol in TMGN-500 (50 mM Tris-HCL pH8, 10 mM MgCl₂, 500 mM NH₄Cl, and 10% to 40% glycerol). Each glycerol fraction was layered sequentially from most concentrated to least concentrated in a 5ml Beckmann Ultra-Clear open top tube. The RNase P preparation was layered onto these gradients which were subjected to centrifugation at 95,000g for 10.5 hours in a Beckmann SW 55 Ti rotor. After centrifugation 100µl fractions were removed from the top of the gradient. 100µl of fraction 44 was loaded onto glycerol gradient “A”. 350µl of fraction 44 was loaded onto gradients “E”, “F”, and “G”.

***In vitro* transcription of premature transfer RNA**

RNA transcripts of *Bacillus subtilis* premature tRNA^{asp} (pre-tRNA^{asp}) were generated by run-off transcription from the T7 promoter upstream of the pre-tRNA^{asp} gene on plasmid pDW128. Termination of transcription at the appropriate site was achieved by cleaving pDW128 with the restriction enzyme BstNI(Promega) prior to its use in transcription. Run-off transcripts were made with ³²P labeled nucleotide as necessary. Transcription products were gel purified in 6% polyacrylamide urea gels, fractionated, passively eluted into 10mM Tris pH 8, 1mM EDTA and 0.1% SDS buffer, phenol-chloroform extracted, and ethanol precipitated. Pelleted transcripts were re-

suspended in filtered water. P^{32} labeled nucleotide was incorporated into transcription reactions as necessary.

RNase P activity assays

Glycerol gradient fractions were assayed for the ability to cleave ^{32}P -GTP labeled pre-tRNA^{asp} *in vitro*. RNase P assay reactions contained 3 μ l of glycerol gradient fraction, RNase P Assay buffer (100mM ammonium acetate, 25mM MgCl₂, 0.05% nonidet P-40, and 50mM tris), 6000cpm of ^{32}P labeled substrate (pre-tRNA^{asp}) and water up to 10 μ l. This reaction mixture was incubated for five minutes at room temperature. Reaction products were resolved on a 12% polyacrylamide urea gel. Bands were quantified using a phosphorimager, and the percent cleavage for each fraction was calculated from substrate and product band intensities.

SDS-PAGE analysis and gel purification

Every third active fraction from glycerol gradient “A” was precipitated by adding two volumes of acetone to each fraction and incubating at $-20^{\circ}C$ overnight. Precipitated proteins were pelleted at 15,000g for 25 minutes, the acetone removed by decanting and evaporation, and the pellet was re-suspended in 2X protein loading dye (200mM DTT, 4% SDS, 20% glycerol, and 0.1% bromophenol blue). The protein solution was then heated to $95^{\circ}C$ for five minutes before loading onto an SDS-Polyacrylamide gel for analysis. The SDS-PAGE gel was then stained using Bio-Rad silver staining reagents.

All active fractions from glycerol gradients “E”, “F”, and “G” were pooled and dialyzed in 10mM Tris-HCl, pH8. This dialyzed material was then precipitated with 3 volumes of acetone overnight at $-20^{\circ}C$. The proteins were pelleted at 25,000g for 25 minutes and the acetone removed by evaporation. The protein pellet was resuspended in

20µl of 2X protein loading dye and loaded into a single lane on a SDS-polyacrylamide gel. The resulting gel was stained using Gel-Code® Blue Coomassie G-250 based staining reagent (Pierce). All visible protein bands were excised and stored at 4°C.

Protein analysis and identification

MALDI-TOF mass spectrometric analysis was performed on in-gel protein bands digested with trypsin. This procedure was performed by the Protein/DNA Technology Center at Rockefeller University, New York, NY. Analysis of the mass spectra was performed using ProFound peptide mass matching program, found at http://129.85.19.192/profound_bin/WebProFound.exe, against the NCBI-nr archaeal database using monoisotopic conditions and allowing one miscleavage to match actual peptide masses with predicted masses for archaeal proteins in a theoretical trypsin digest.

RESULTS AND DISCUSSION

All glycerol gradients performed using fraction 44 displayed the expected peak of RNase P activity in the middle of the gradient (an example is given in Figure 1). The silver stain gel performed on acetone precipitated active fractions from glycerol gradient “A” showed possibly 8 bands that correlate with RNase P activity(Figure 2). The estimated molecular weights of these bands were 14.1kDa, 21.1kDa, 22.9kDa, 34.3kDa, 36.3kDa, 38.9kDa, 47.8kDa, 66.1kDa, and 83.2kDa.

Active fractions that were pooled and dialyzed overnight in buffer also retained the ability to cleave pre-tRNA *in vitro* (Figure 1). The gel run with the dialyzed material from gradients “E”, “F”, and “G” also showed these same bands when stained with Coomassie G-250, but additional bands appeared as well (Figure 3). It is important to note that bands correlating to RNase P activity stained with differing intensity depending

which stain was used. MJ-4 was the darkest of the bands excised, indicating a concentration closer to that of the molecular weight markers. Other protein bands were barely visible indicating a concentration closer to the sensitivity of the Coomassie blue stain (8ng). A total of 15 protein bands were excised (labeled MJ-1 through MJ-15), 11 of which were analyzed by MALDI-TOF mass spectrometry depending on their estimated size when compared to the silver stain gel.

Of the eleven protein bands analyzed, 9 had peptide-mass fingerprint spectra that could be matched to hypothetical *M. jannaschii* proteins. The spectra of each protein band can be seen in Figures 4 through 12 with the corresponding ProFound search results below them, excluding band MJ-3a which produced no spectrum. The bands and the proteins identified via the ProFound search are as follows: MJ-2 is MJ1625, MJ-3 is MJ0376, MJ-4 is MJ1139, MJ-8 is MJ1128, MJ-9 is *M. jannaschii* 30S ribosomal protein S8E, MJ-10 is *M. jannaschii* 30S ribosomal protein S6E, MJ-12 is MJ0541 and MJ0464, MJ-13 is MJ0464, and MJ-14 is MJ0332.1. MJ-11 and MJ-3a could not be identified. A summary of the mass spectrometry fingerprint analysis can be seen in Table 1.

Six of the mass peaks produced from digestion of MJ-4 matched to masses for theoretically digested MJ1139. The remaining bands had less than 5 matched hits which is as a standard too few to confirm the identity of a protein. However, due to the low amount of protein used in this analysis and low cleavage efficiency, it is possible that some bands did not appear on the mass spectra fingerprint. MJ-2 and MJ-3 both produced spectra corresponding to conserved hypothetical proteins. MJ-2 produced a spectra of five defined peaks, 2 of which had masses matching predicted peptide masses in MJ1625. The spectrum produced from a trypsin digest of MJ-3 resulted in 30 mass

peaks that were used in a ProFound search matching 4 masses to peptide masses of MJ0376. Both of these identified proteins are conserved amongst the Archaea and are possible *M jannaschii* RNase P proteins.

MJ-9, MJ-10 and MJ-12 are unique in that they were previously identified as gene products. MJ-9 and MJ-10 were identified to be 30S ribosomal protein subunits, S8E(MJ0673) and S6E(MJ1260) respectively, both of which belong to a highly conserved family of ribosomal proteins. Because ribosomal components are difficult to separate from RNase P even in Cs_2SO_4 gradients, a key step in purification of the enzyme, it is possible to get ribosomal protein contamination. However, it is also feasible that RNase P shares subunits with the ribosome. In yeast RNase P, eight of the nine proteins identified are shared with a ribosomal RNA processing enzyme, RNase MRP (2). MJ-12 peptide masses matched *M. jannaschii* nicotinamide-nucleotide adenylyltransferase (MJ0541).

Analysis of archaeal genomes has shown that most of the components involved in translation, transcription, and replication resemble their eukaryotic relatives more so than those seen in the Bacteria (10). Other components of the archaeal cell involved in cell structure and metabolic pathways more generally resemble those of their Bacterial relatives. It is possible that the Archaea share this same motif of protein cofactor overlap between enzymes involved in macromolecular synthesis as seen in the Eukaryotes. This theme of gene resemblance supports that MJ1260 is a possible RNase P protein due to its role in translation, and supports that MJ0541 is a contaminant because it is a metabolic enzyme. MJ0541 could be an RNase P modification enzyme explaining its presence in purified extracts of *M. jannaschii* RNase P.

MJ-12 also contains peptide masses matching those predicted for a trypsin digest of MJ0464. The mass spectrum fingerprint from MJ-13 also revealed peptide masses corresponding to the same theoretical peptide masses from MJ0464 that match in MJ-12. This could indicate that M0464 exists as two forms in the cell, modified or unmodified. The estimated molecular weight of MJ0464 agrees with the positioning of either MJ-12 or MJ-13 due to the close proximity of these bands in the gel. MJ-14 paired with hypothetical protein MJ0332.1 with only two matches of 12 possible peptide masses, and though it is a possible that this is an RNase P protein, the molecular weight of this protein is slightly high for its gel position and may have been identified in error.

Though it has been shown that archaeal RNase Ps have multiple protein subunits, the reason for having so many is unknown. For Bacteria, one protein subunit is sufficient for cleaving pre-tRNA *in vivo* and the *in vitro* cleavage reaction is possible without protein entirely (5). One role of the protein is to shield electrostatic interactions between the RNAs involved in the cleavage reaction allowing binding of one negative nucleic acid to another (4). This is certainly supported by the *in vitro* substitution of divalent and monovalent cations in the ribozyme reaction for protein. Other roles for the protein have been suggested for the bacterial protein subunits. Interactions of bacterial protein subunits with substrates including pre-tRNA, mature tRNA, and 4.5S RNA indicate that the protein has substrate discriminating ability as well as a possible RNA melting function to facilitate product release (7,12,14).

The RNA component of archaeal RNase P is very similar in secondary structure to that of their bacterial counterparts and some archaeal RNAs possess ribozyme activity at very high ionic strength (6,13). *M. thermoautotrophicus* RNase P RNA is a type A

RNA and has ribozyme activity and presumably would only need the protein subunit for activity as observed in the Bacteria and for the same reasons (6,13). *M. jannaschii*, on the other hand, has an RNase P RNA of type M that can not cleave substrate *in vitro* without its associated proteins (6,13). Type M RNAs lack certain secondary structures that are important for substrate binding and do not have extra structure to recover this role. One proposed role for the extra protein subunits found associated with type M RNAs could be to compensate for the missing substrate binding secondary structure elements.

Here we have established that MJ1139 is present in highly purified extracts of RNase P from *M. jannaschii*. This data also suggests that MJ0464 is present, although at lower concentrations, in the RNase P holoenzyme and possibly in several forms. Other proteins identified as potential RNase P subunits are MJ1625, MJ0376, and the 30S ribosomal subunit S6E.

Protein Band	Identified Protein	Annotated Protein Function	Number of Peaks Matched	Number of Peaks	% Sequence Covered	Estimated Exp. Mol Weight	Theoretical Molecular Weight (kDa)
2	MJ1625	conserved hypothetical protein	2	5	2	94 - 67	78.60
3	MJ0376	conserved hypothetical protein	4	30	6	94 - 67	86.22
3A	-----	-----	-----	-----	-----	50 - 43	-----
4	MJ1139	RNase P subunit	6	19	31	30	27.33
8	MJ1128	hypothetical protein	2	2	10	14-30	34.4
9	MJ0673	SSU ribosomal protein S8E	4	7	22	20-30	14.52
10	MJ1260	SSU ribosomal protein S6E	2	12	20	20 - 14.4	14.35
11	-----	-----	-----	-----	-----	-----	-----
12	MJ464	RNase P subunit	3	19	32	20 - 14.4	10.87
	MJ0541	nicotinamide-nucleotide adenylyltransferase	4	19	21		19.59
13	MJ464	RNase P subunit	3	14	32	20 - 0	10.87
14	MJ0332.1	hypothetical protein	2	12	20	20 - 0	14.95

Table 1. Summary of analysis of protein bands numbered in Figure ?. Analysis was performed using ProFound (http://129.85.19.192/profound_bin/WebProFound.exe) which searches protein databases for predicted peptide masses that match experimental peptide masses.

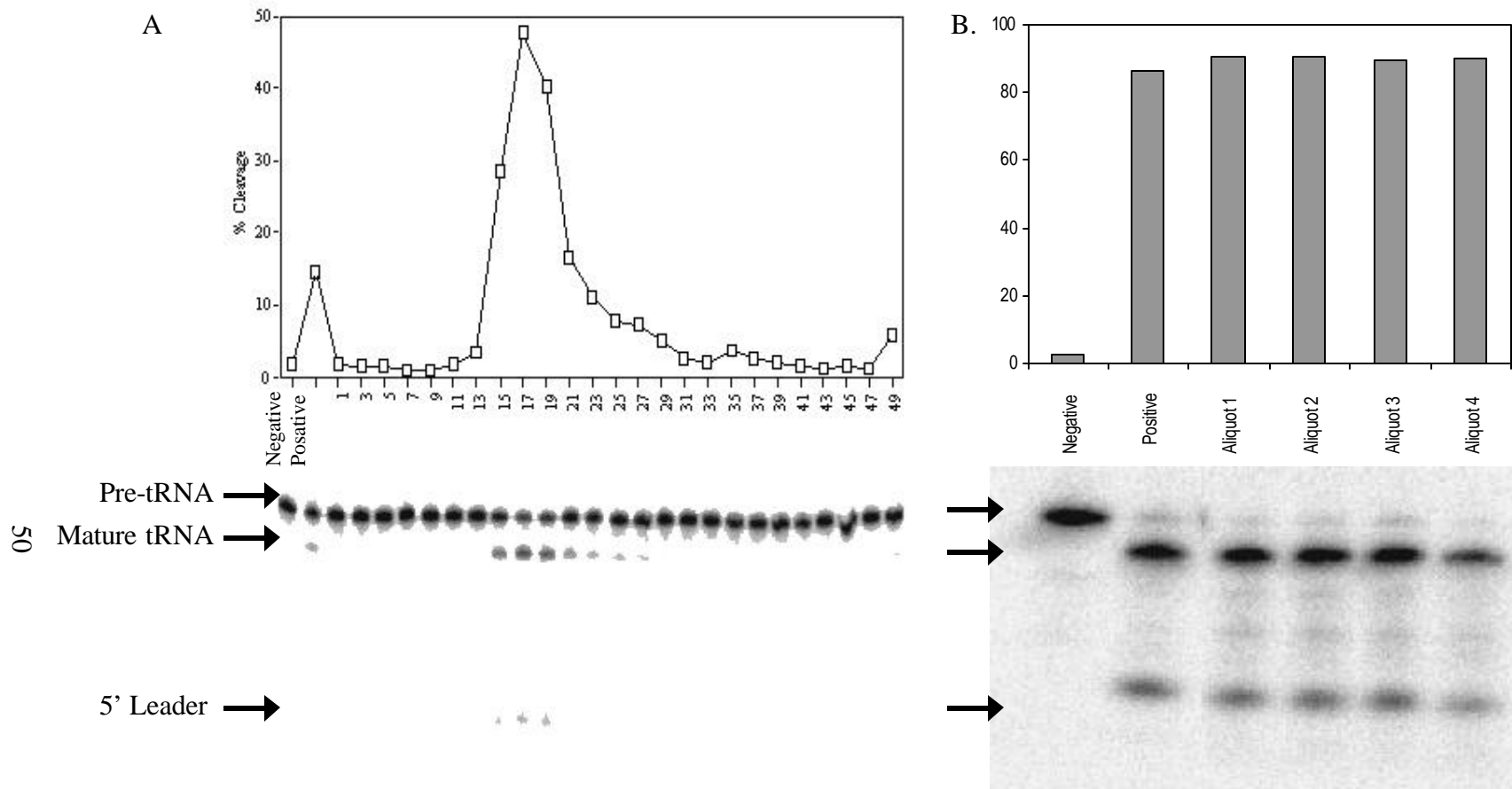


Figure 1. RNase P activity assays. (A) Every odd fraction from glycerol gradient "G" was tested for the ability to cleave radiolabelled pre-tRNA substrate. (B) After dialysis the RNase P-containing fraction retained the ability to cleave substrate. Reaction products are indicated by arrows. Fractions were dialyzed and aliquotted into four tubes. Lanes 5-8 contained 1ul of dialyzed RNase P from the aliquots 1-4 respectively. Lanes 1 and 2 are the controls, the negative reaction containing substrate only and the positive reaction containing 1ul of "fraction #44".

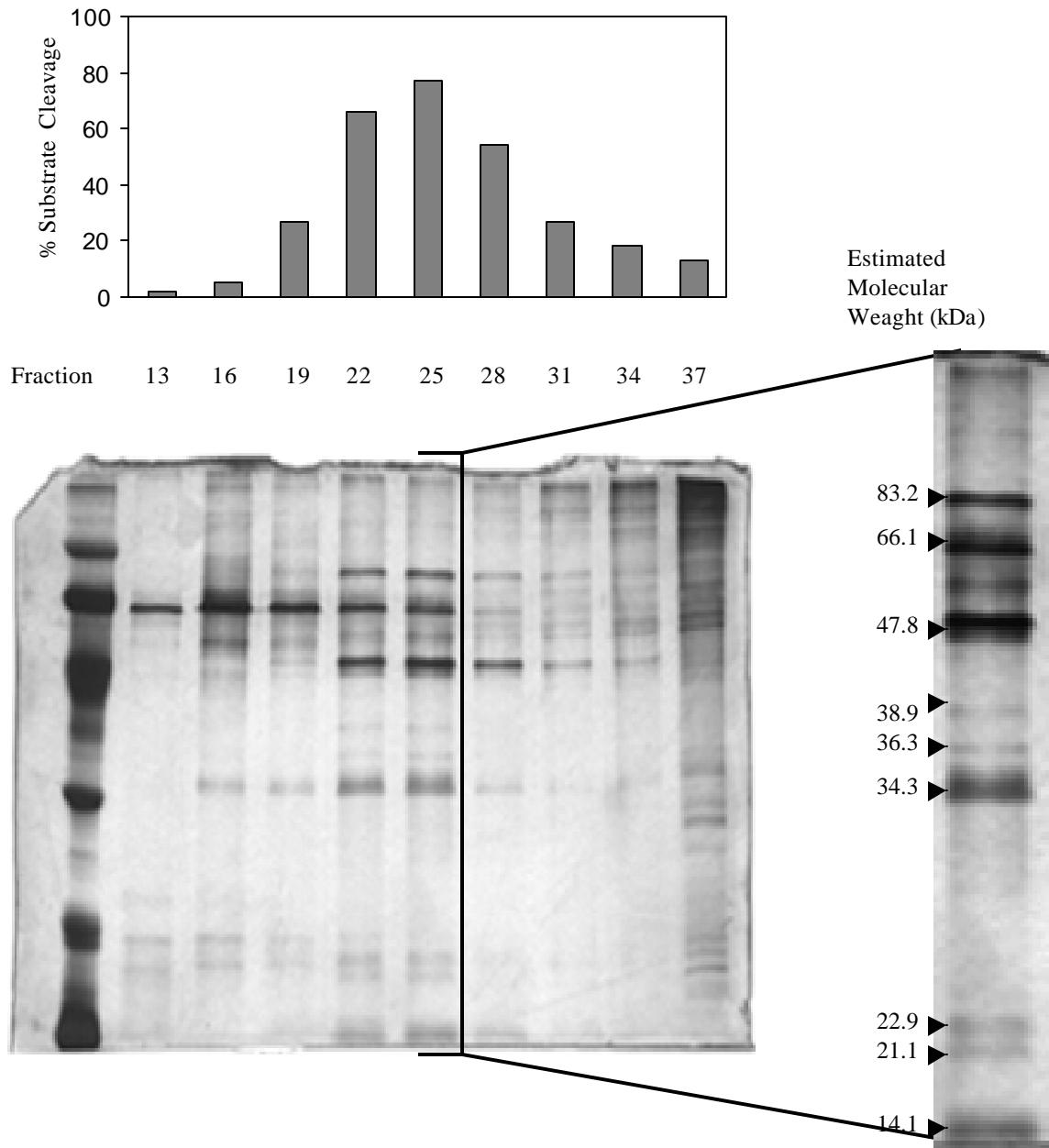


Figure 2. Glycerol gradient fractions with RNase P activity. Every third fraction starting with fraction 13 and ending with fraction 37 was tested for its ability to cleave radiolabelled substrate, was acetone precipitated, and analyzed via SDS-PAGE. Shown here is that silver stained gel with the percent substrate cleavage corresponding to each fraction shown above and the fraction exhibiting the most activity has been enlarged to the right. The estimated molecular weights of protein bands of interest are shown beside them in the enlarged view.

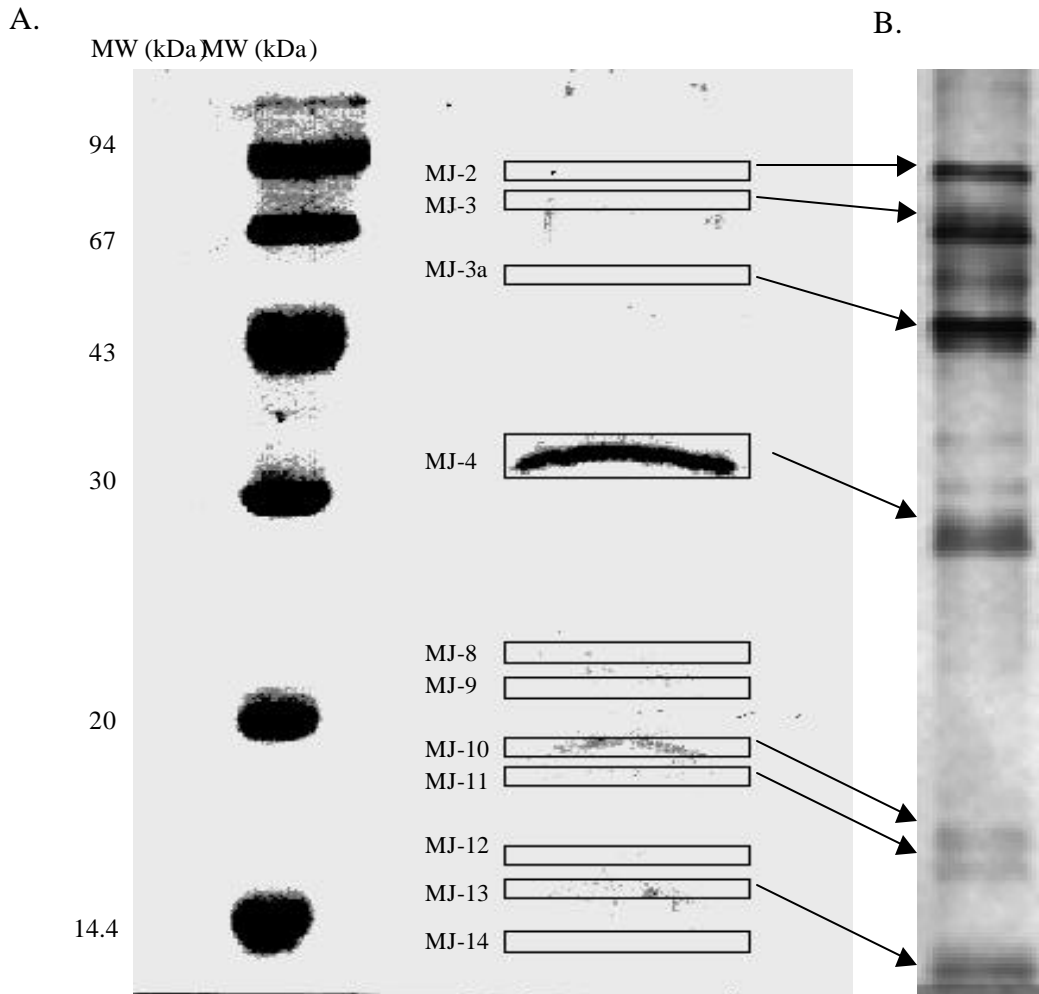
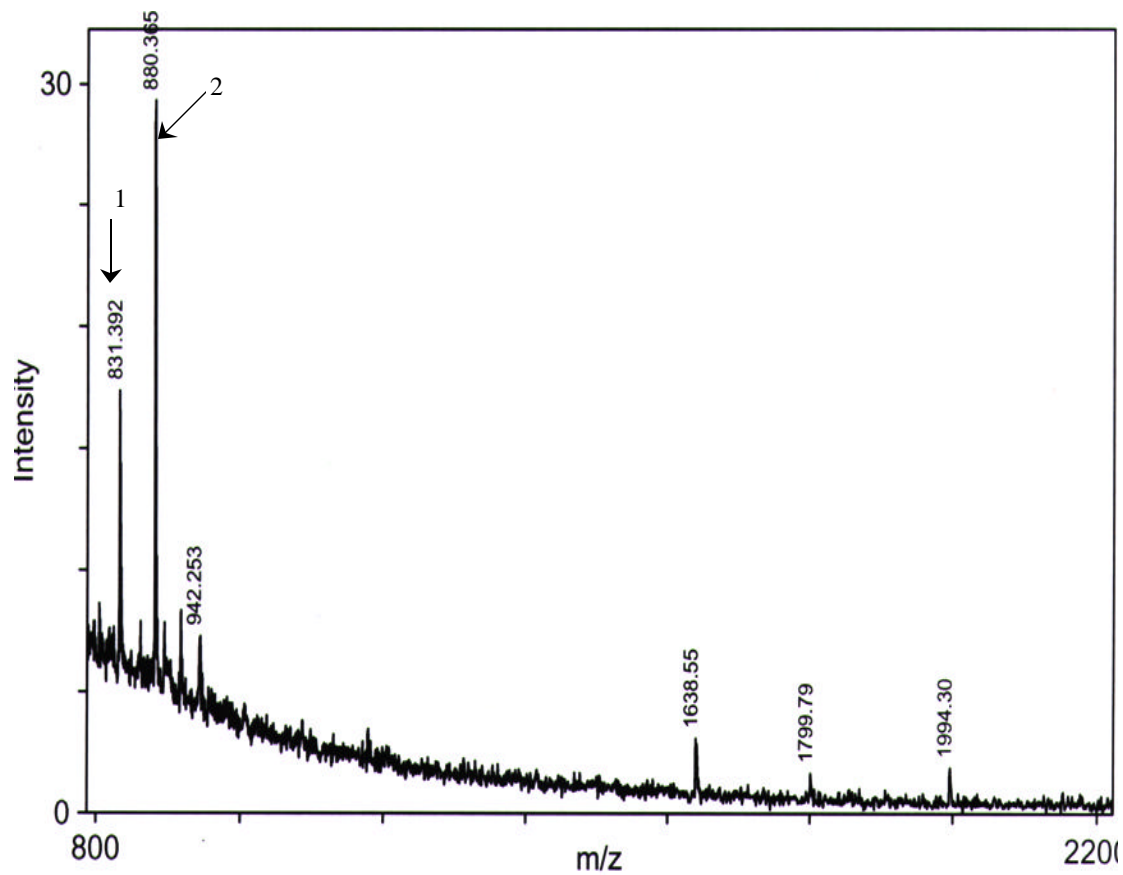
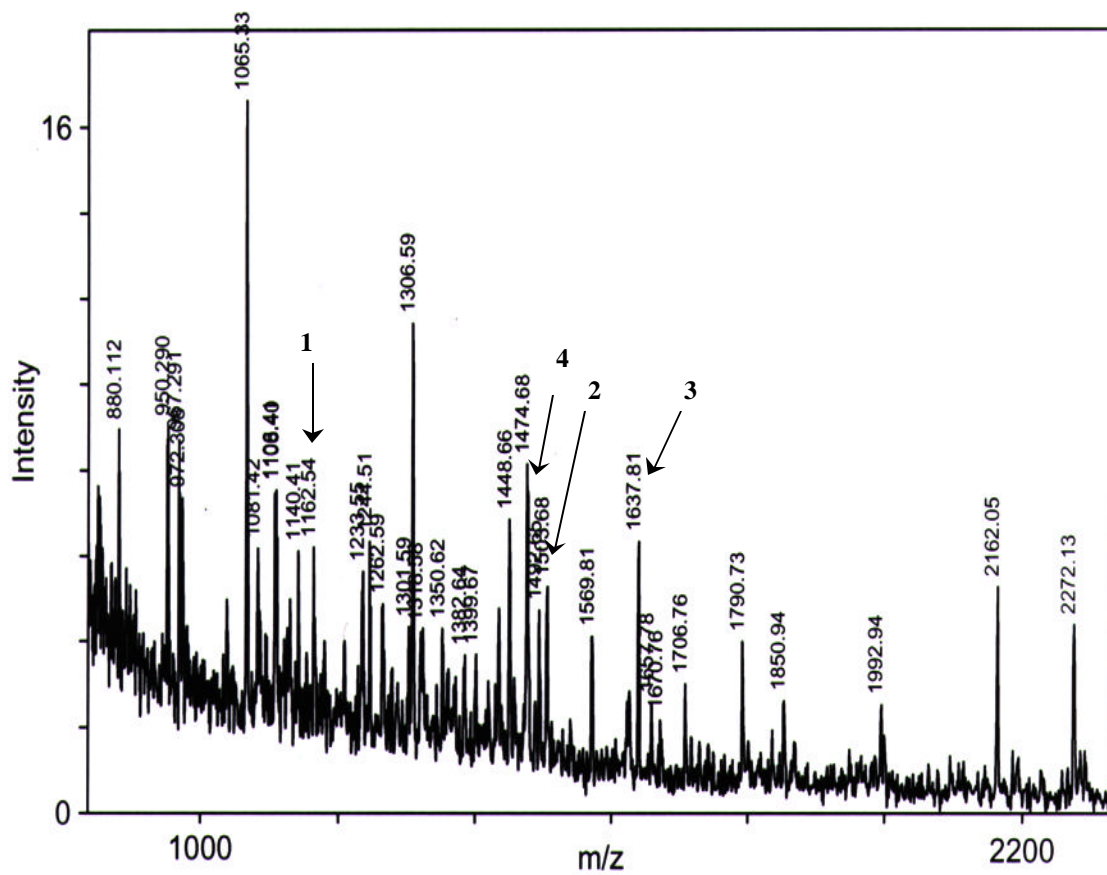


Figure 3. (A) SDS-PAGE analysis of glycerol gradients "E", "F", and "G" fractions exhibiting RNase P activity (lane 2). Numbered and boxed protein bands were excised, digested with trypsin, and analyzed further by MALDI-TOF mass spectrometry. Protein markers in lane 1 have their molecular weights adjacent to each band. Fractions were dialyzed prior to gel loading and this gel was stained using Peirce gel-code blue Coomassie G-250 staining reagent. Adjacent (B) is the peak fraction of glycerol gradient "A" run in SDS-PAGE and silver stained.



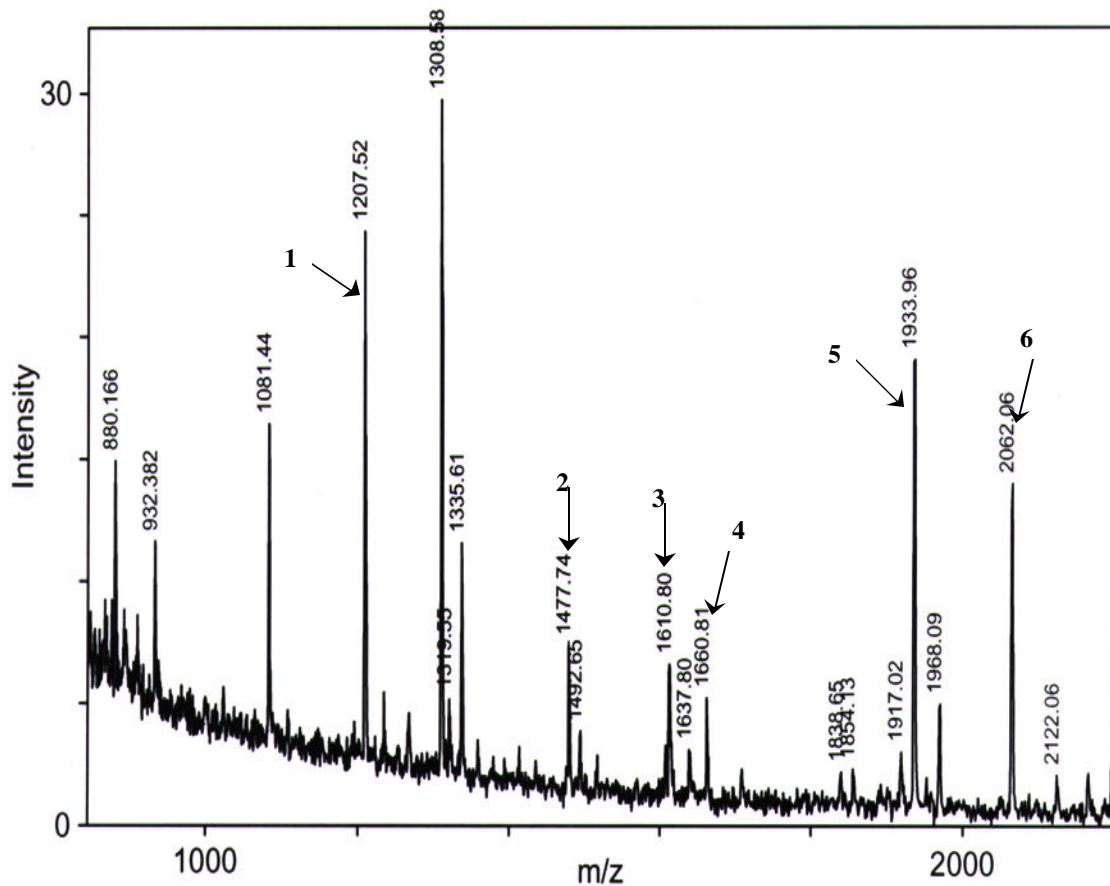
Peak	Measured mass	Calculated mass	Error	Residues	Number of miscuts	Peptide sequence
1	831.392	831.433	-0.041	451-457	1	KGEEELK
2	880.365	880.414	-0.049	460-466	1	ESMQMKK

Figure 4. MALDI-TOF peptide-mass fingerprint spectrum of the trypsin digest of gel slice MJ-2 (top). This protein band was identified to be MJ1625. Peaks corresponding to predicted peptide masses in a theoretical trypsin digest of *M. jannaschii* hypothetical protein 1625 are indicated by numbered arrows, and data corresponding to the matches are summarized in the table (bottom).



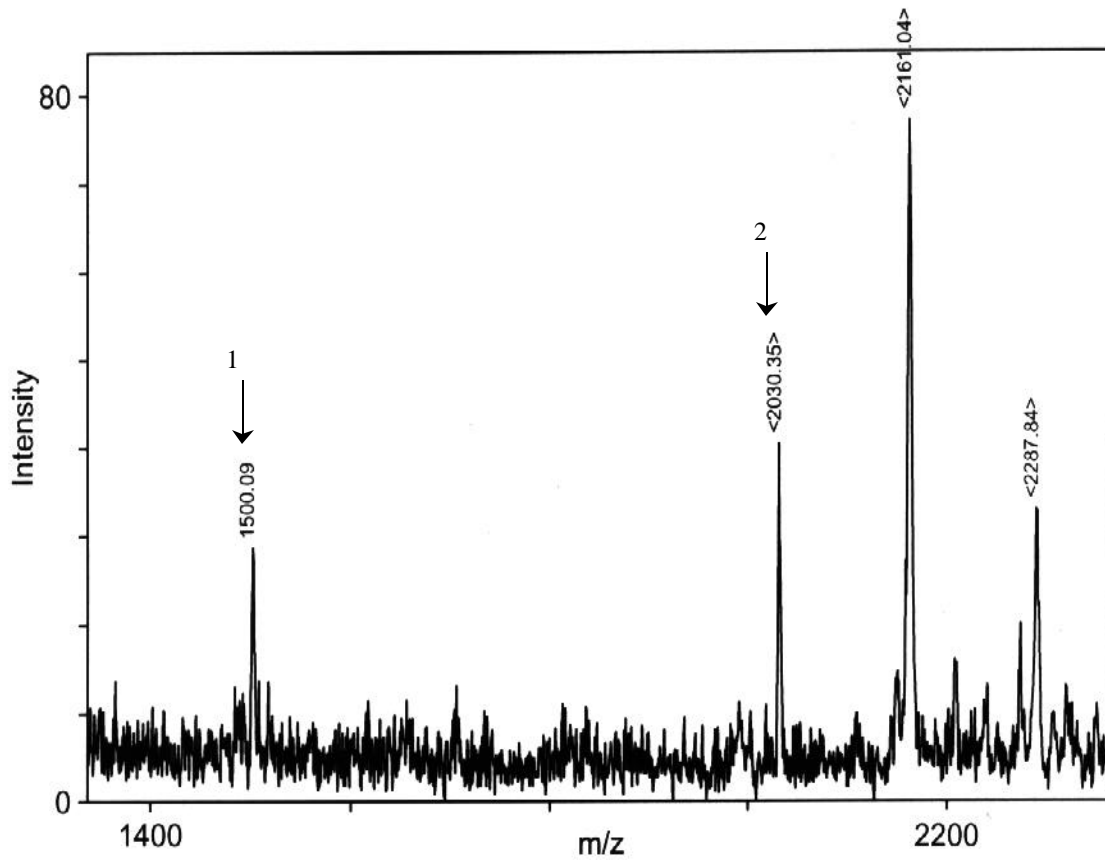
Peak	Measured Mass	Calculated Mass	Error	Residues	Number of Miscuts	Peptide sequence
1	1162.540	1162.598	-0.058	7-16	0	ITEG FQNNIK
2	1503.680	1503.657	0.023	294-305	0	EIEDE DDLEEI R
3	1637.810	1637.772	0.038	682-694	0	NEEGL IHFYP YEK
4	1492.650	1492.732	-0.073	95-106	1	GFSKFFEFDLK

Figure 5. MALDI-TOF peptide-mass fingerprint spectrum of the trypsin digest of gel slice MJ-3. This protein band was identified to be MJ0376. Peaks corresponding to predicted peptide masses in a theoretical trypsin digest of *M. jannaschii* hypothetical protein 0376 are indicated by numbered arrows in the spectrum, and data corresponding to the matches are summarized in the table (bottom). Calibration peaks can be seen with masses of 2162.05 and 2272.1.



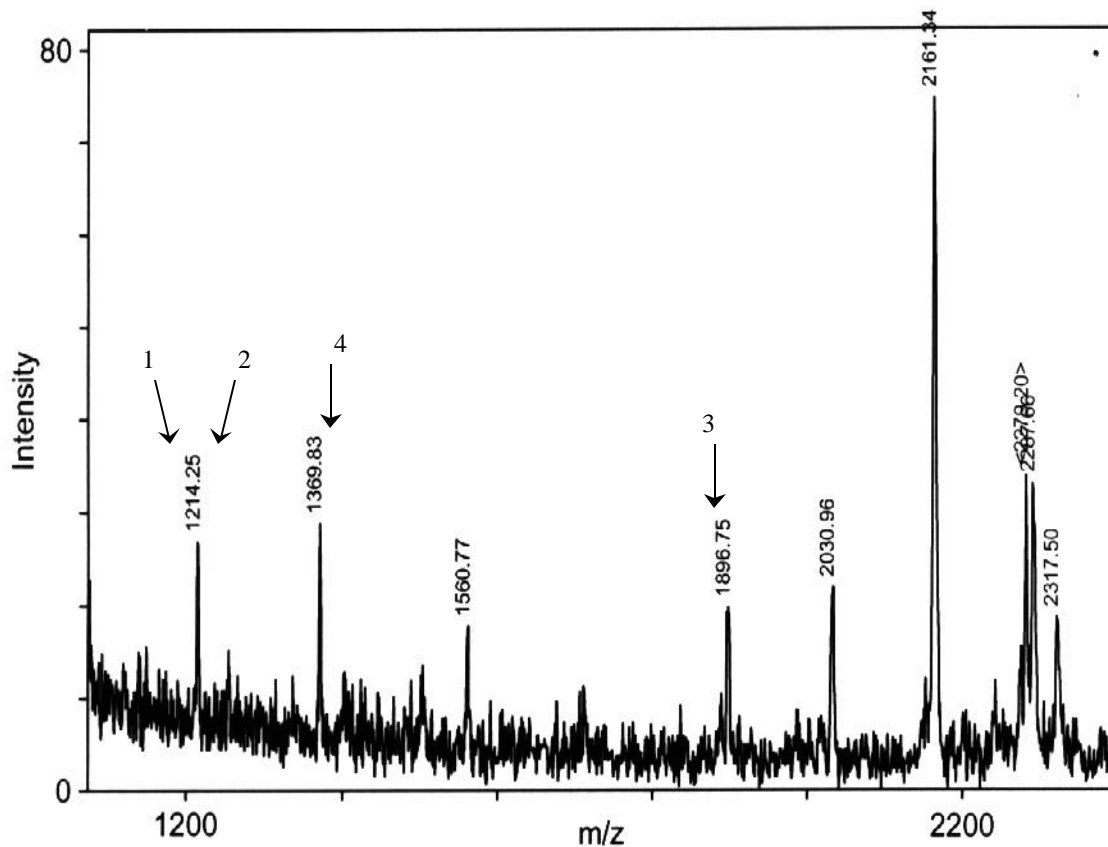
Peak	Measured Mass	Calculated Mass	Error	Residues	Number of Miscuts	Peptide sequence
1	1207.520	1207.619	-0.099	136-145	1	TLLNKDGYER
2	1477.740	1477.817	-0.078	186-198	0	AFLNTLVEPLY AK
3	1610.800	1610.889	-0.089	122-135	1	LASNHRVAIELNFK
4	1660.810	1660.866	-0.057	161-175	1	KFDVPVVISDAENK
5	1933.960	1934.010	-0.050	93-110	0	AAVELHDVDILSTPELGR
6	2062.060	2062.105	-0.045	93-111	1	AAVELHDVDILSTPELGRK

Figure 6. MALDI-TOF peptide-mass fingerprint spectrum of the trypsin digest of gel slice MJ-4 (top). This protein band was identified to be MJ1139, a predicted RNase P protein. Peaks corresponding to predicted peptide masses in a theoretical trypsin digest of *M. jannaschii* hypothetical protein 1139 are indicated by numbered arrows, and data corresponding to the matches are summarized in the table (bottom).



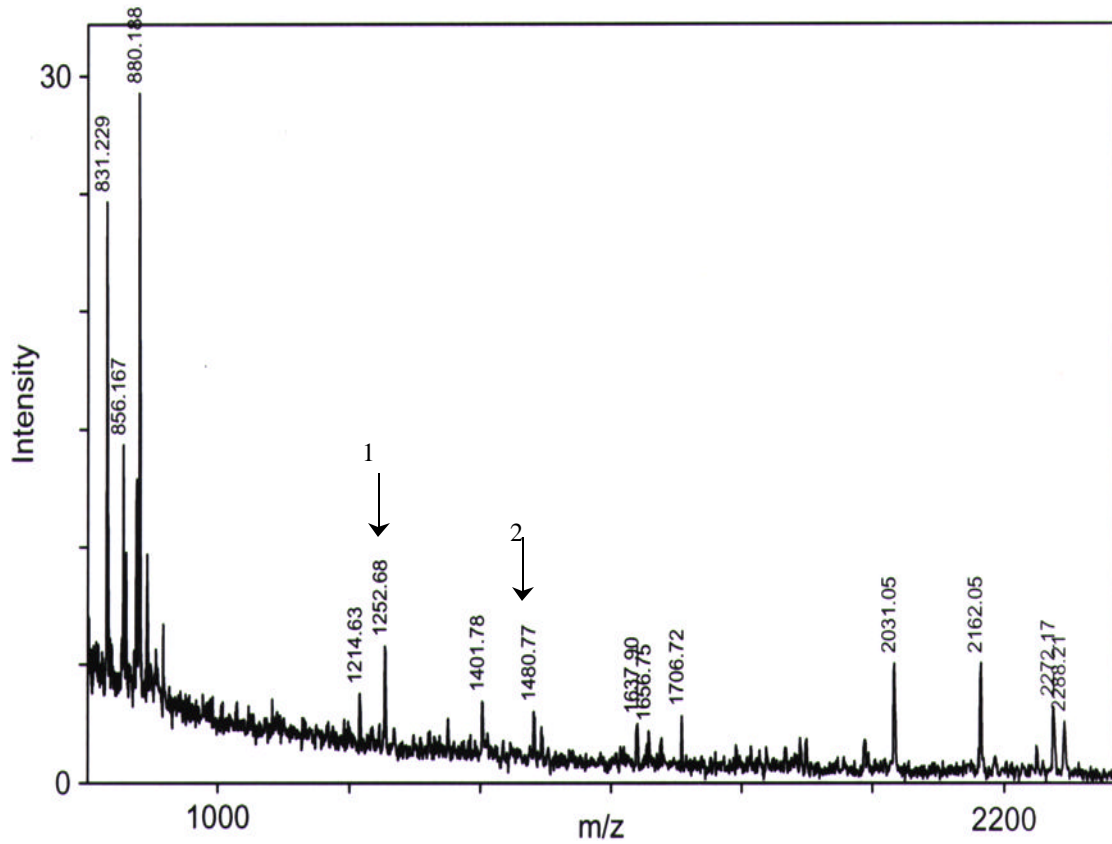
Peak	Measured Mass	Calculated Mass	Error	Residues	Number of Miscuts	Peptide Sequence
1	1500.090	1500.709	-0.619	161-173	0	TLYLAYEATGDER
2	2030.350	2031.016	-0.667	67-83	1	YIGYQITPHNVNEEARK

Figure 7. MALDI-TOF peptide-mass fingerprint spectrum of the trypsin digest of gel slice MJ-8 (top). This band was identified to be *M. jannaschii* hypothetical protein MJ1128. Peaks corresponding to predicted peptide masses in a theoretical trypsin digest of MJ1128 are indicated by numbered arrows in the spectrum, and data corresponding to the matches are summarized in the table (bottom). Calibration peaks can be seen with masses of 2161.04 and 2287.84.



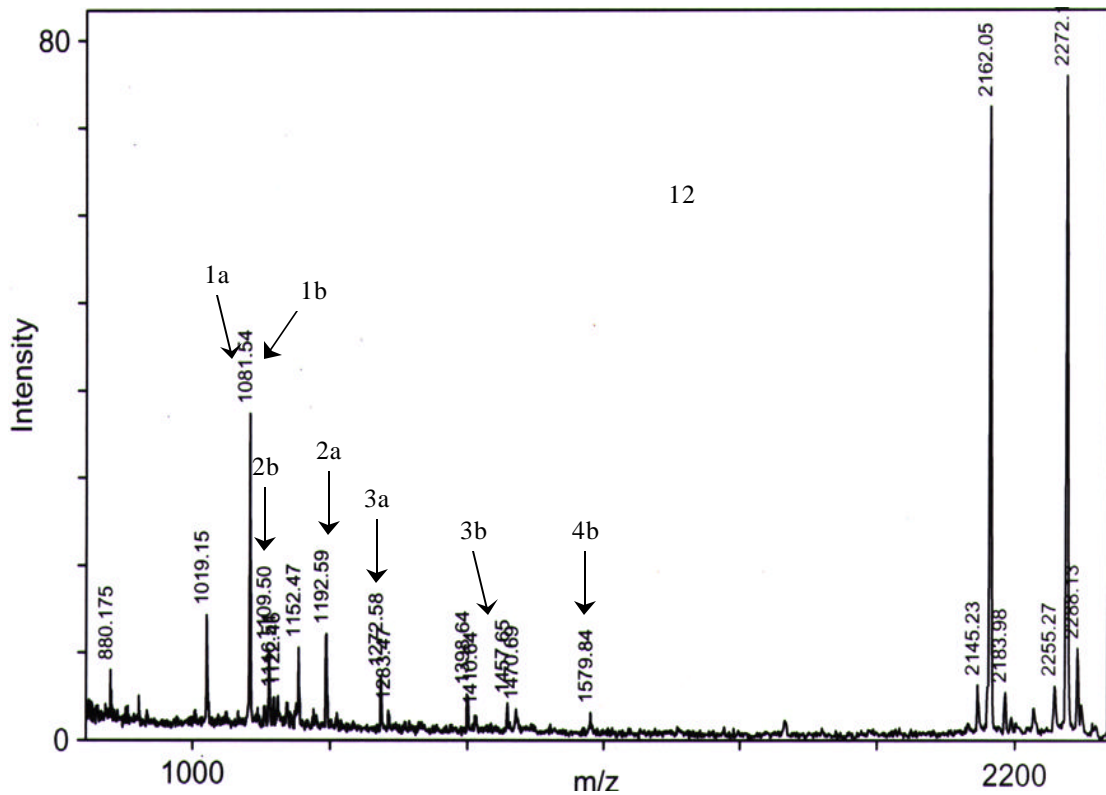
Peak	Measured Mass	Calculated Mass	Error	Residues	Number of Miscuts	Peptide Sequence
1	1214.250	1214.688	-0.438	11-12	0	KPTGGLYRPAR
2	1214.250	1213.691	0.559	100-111	0	GAIHETEIGLAK
3	1369.830	1370.789	-0.959	10-21	1	RKPTGGLYRPAR
4	1896.750	1897.026	-0.276	112-129	1	VTSRPGQDGTVNAILIKE

Figure 8. MALDI-TOF peptide-mass fingerprint spectrum of the trypsin digest of gel slice MJ-9 (top). This band was identified to be MJ0673. Peaks corresponding to predicted peptide masses in a theoretical trypsin digest of *M. jannaschii* 30S ribosomal protein S8E (MJ0673) are indicated by numbered arrows in the spectrum, and data corresponding to the matches are summarized in the table (bottom). Calibration peaks can be seen with masses of 2161.31 and 2279.20.



Peak	Measured Mass	Calculated Mass	Error	Residues	Number of Miscuts	Peptide sequence
1	1252.680	1252.754	-0.074	72-83	0	VLLSAPPGFKPK
2	1480.770	1480.824	-0.054	95-108	0	GNTIAPDIVQINVK

Figure 9. MALDI-TOF peptide-mass fingerprint spectrum of the trypsin digest of gel slice MJ-10 (top). This band was identified to be MJ1260. Peaks corresponding to predicted peptide masses in a theoretical trypsin digest of *M. jannaschii* 30S ribosomal protein S6E (MJ1260) are indicated by numbered arrows in the spectrum, and data corresponding to the matches are summarized in the table (bottom). Calibration peaks can be seen with masses of 2162.05 and 2272.17.



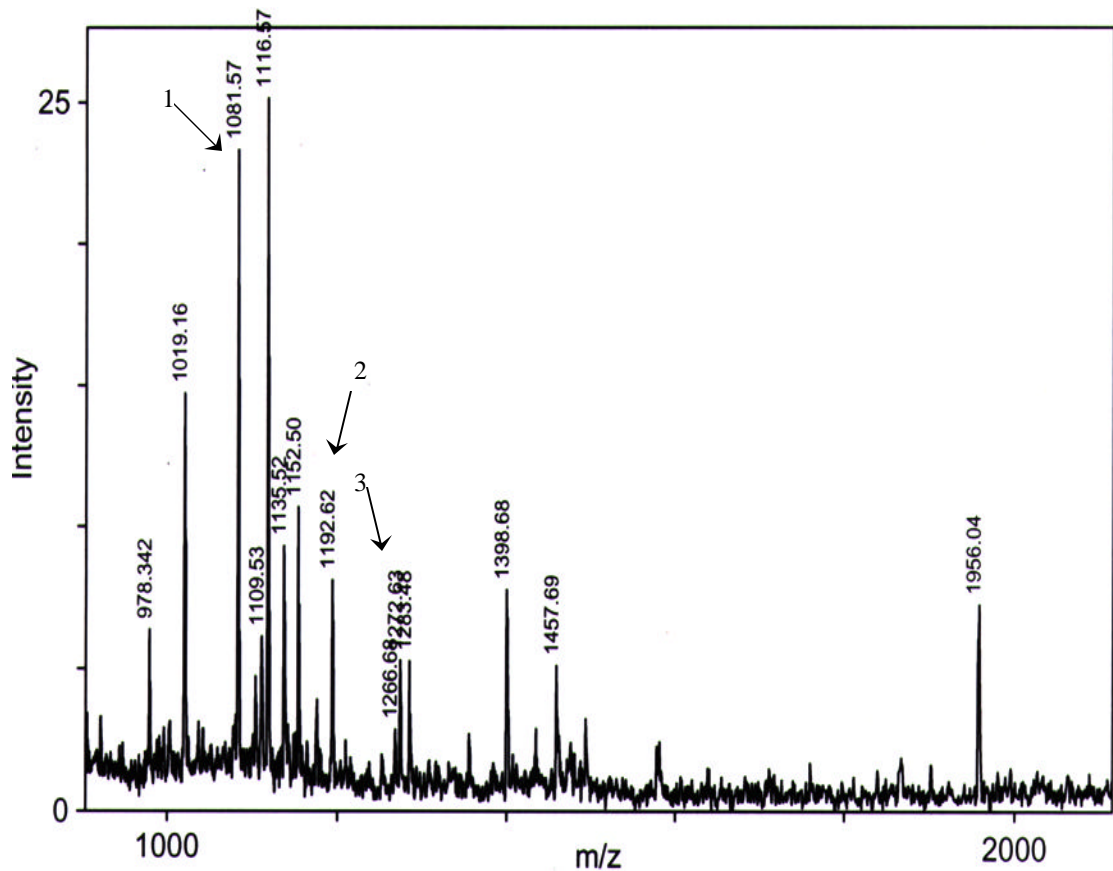
A.

Peak	Measured mass	Calculated mass	Error	Residues	Number of miscuts	Peptide sequence
0541						
1a	1081.540	1081.624	-0.084	76-84	0	LLIGRPEER
2a	1192.590	1192.685	-0.095	57-66	0	DIAVFLFQLK
3a	1272.580	1272.667	-0.087	40-50	1	NTLVIEKEDGR

B.

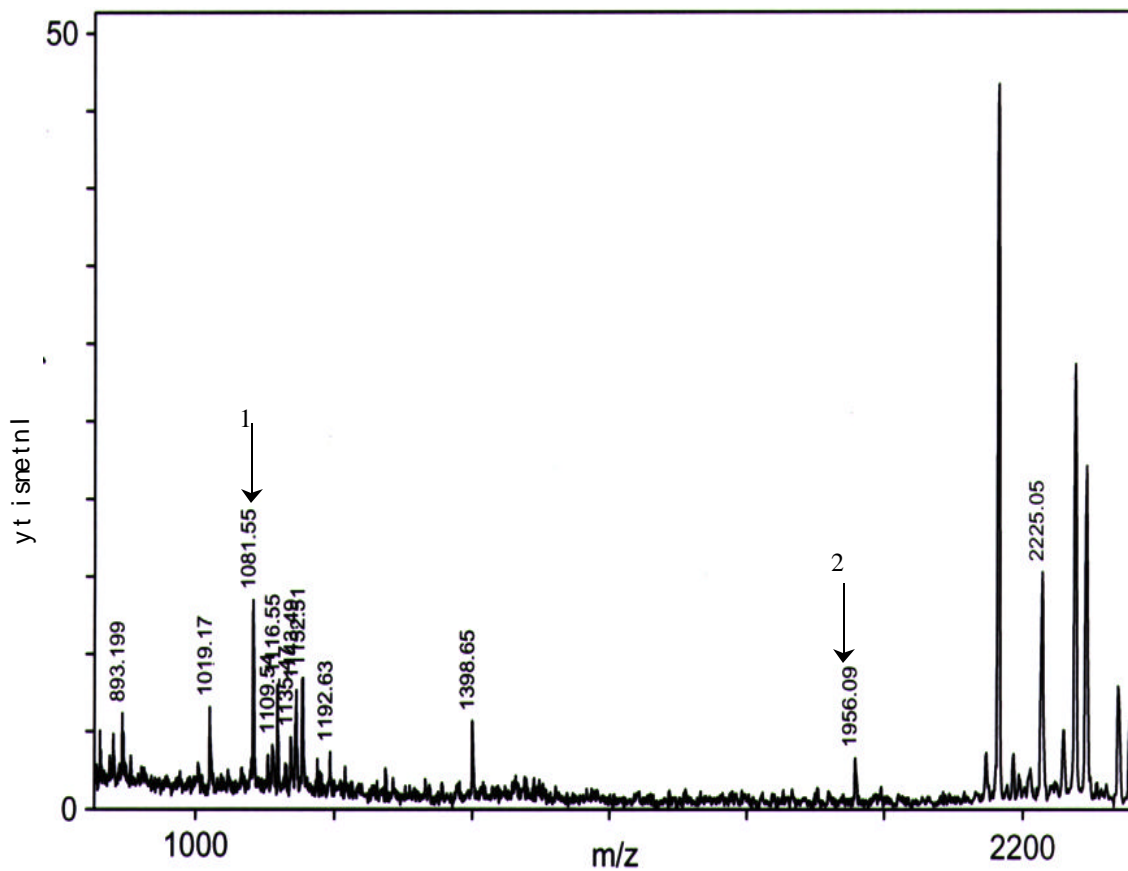
Peak	Measured mass	Calculated mass	Error	Residues	Number of miscuts	Peptide sequence
0464						
1b	1081.540	1081.540	0.000	122-130	1	KEYSGTEIR
2b	1109.500	1109.546	-0.046	123-131	1	EYSGTEIRR
3b	1457.650	1457.689	-0.039	40-52	0	SHTLENPFTAGER
4b	1579.840	1579.817	0.023	133-145	1	MLNGEKWEHLVPK

Figure 10. MALDI-TOF peptide-mass fingerprint spectrum of the trypsin digest of gel slice MJ-12 (top). This band was identified to be one or both of two proteins, MJ 0541 and MJ0464. Peaks corresponding to predicted peptide masses in a theoretical trypsin digest of *M. jannaschii* hypothetical proteins 0541(nicotinamide-nucleotide adenylyltransferase) and 0464 are indicated by numbered arrows, and data corresponding to the matches are summarized in the tables A. and B respectively (bottom). Calibration peaks can be seen with masses of 2162.05 and 2272.1.



Peak	Measured mass	Calculated mass	Error	Residues	Number of miscuts	Peptide sequence
1	1081.570	1081.624	-0.054	76-84	0	LLIGRPEER
2	1192.620	1192.685	-0.065	57-66	0	DIAVFLFQLK
3	1272.630	1272.667	-0.037	40-50	1	NTLVIEKEDGR

Figure 11. MALDI-TOF peptide-mass fingerprint spectrum of the trypsin digest of gel slice MJ-13 (top). This band was identified to be MJ0464, a predicted RNase P protein. Peaks corresponding to predicted peptide masses in a theoretical trypsin digest of *M. jannaschii* hypothetical protein 0464 are indicated by numbered arrows, and data corresponding to the matches are summarized in the table below (bottom).



Peak	Measured mass	Calculated mass	Error	Residues	Number of miscuts	Peptide sequence
1	1081.550	1081.453	-0.001	109-118	1	ISGRSSNSFK
2	1956.090	1956.073	0.017	60-75	1	KAVPYVINYFKPPHQR

Figure 12. MALDI-TOF peptide-mass fingerprint spectrum of the trypsin digest of gel slice MJ-14 (top). This band was identified to be MJ0332.1. Peaks corresponding to predicted peptide masses in a theoretical trypsin digest of *M. jannaschii* hypothetical protein 0332.1 are indicated by numbered arrows, and data corresponding to the matches are summarized in the table below (bottom).

REFERENCES

Andrews, A. J., Hall, T.A., and J.W. Brown. 2001. RNase P in methanogenic Archaea. *J. Biol. Chem.* Accepted 6-15-01.

Chamberlain, J.R., Lee, Y., Lane, W.S., and D.R. Engelke. 1998. Purification and characterization of the nuclear RNase P holoenzyme complex reveals extensive subunit overlap with RNase MRP. *Genes and Dev.* 12:1678-1690.

Darr, S.C., B. Pace, and N.R. Pace. 1990. Characterization of ribonuclease P from the archaeobacterium *Sulfolobus solfataricus*. *J. Biol. Chem.* 265:12927-12932.

Frank, D.N. and N.R. Pace. 1998. Ribonuclease P: unity and diversity in a tRNA processing ribozyme. *Annu. Rev. Biochem.* 67:153-180.

Guerrier-Takada, C., K. Gardner, T. Marsh, N. Pace, and S. Altman. 1983. The RNA moiety of ribonuclease P is the catalytic subunit of the enzyme. *Cell* 35:849-857.

Harris, J.K., Haas, E.S., Williams, D., Frank, D.N., and J.W. Brown. 2001. New insight into RNase P structure from comparative analysis of the archaeal RNA. *RNA* 7:220-232.

Kirsebom, L.A. 1995. RNase P--a 'Scarlet Pimpernel'. *Mol. Microbiol.* 17:411-20.

Koonin, E.V., Wolf, Y.I., and L. Aravind. 2001. Prediction of the archaeal exosome and its connections with the proteasome and the translation and transcription machineries by a comparative-genomic approach. *Genome Res.* 11:240-252.

Lawrence, N., Wesolowski, D., Gold, H., Bartkiewicz, M., Guerrier-Takada, C., McClain, W.H., and S. Altman. 1987. Characteristics of ribonuclease P from various organisms. *Cold Spring Harbor Symp. Quant. Biol.* 52:233-238.

Makarova, K.S., Aravind, L., Galperin, M.Y., Grishin, N.V., Tatusov, R.L., Wolf, Y.I., and E.V. Koonin. 2001. Comparative genomics of the Archaea (Euryarchaeota): evolution of conserved protein families, the stable core, and the variable shell. *Genome Res.* 9:608-628.

Nieuwlandt, D.T., Haas, E.S., and C.J. Daniels. 1991. The RNA component of RNase P from the archaeobacterium of *Haloferax volcanii*. *J. Biol. Chem.* 266:5689-5695.

Niranjanakumari, S., Stams, T., Crary, S.M., D.W. Christianson, and C.A. Fierke. 1998. Protein component of the ribozyme ribonuclease P alters substrate recognition by directly contacting precursor tRNA. *Proc. Natl. Acad. Sci.* 95:15212-15217.

Pannucci, J.A., Haas, E.S., Hall, T.A., Harris, J.K., and J.W. Brown. 1999. RNase P RNAs from some Archaea are catalytically active. *Proc. Natl. Acad. Sci.* 96:7803-7808.

Peck-Miller, K.A., and S. Altman. 1991. Kinetics of the processing of the precursor to 4.5 S RNA, a naturally occurring substrate for RNase P from *Escherichia coli*. *J. Mol. Biol.* 221:1-5.

Reich, C., Olsen, G.J., Pace, B., and N.R. Pace. 1988. Role of the protein moiety of ribonuclease P a ribonucleoprotein enzyme. *Science* 239:178-181.

APPENDIX A: CLONING OF THE *PYROCOCCUS FURIOSUS* DNA POLYMERASE GENE

PURPOSE:

Recombinant enzymes such as DNA and RNA polymerases are expensive tools necessary for work in molecular biology. Cloning of the genes corresponding to these enzymes and expression of recombinant protein can be an inexpensive alternative to purchasing the commercially produced enzymes. In particular, the DNA polymerase from *Pyrococcus furiosus* (*Pfu* DNA polymerase) is of interest because it is highly efficient and has superior proof reading activity compared to other thermophilic DNA polymerases and is in addition more expensive than more commonly used DNA polymerases (1). *Pfu* DNA polymerase can be over expressed in *Escherichia coli* to produce large amounts of active enzyme (1). Described here is the method by which *Pfu* DNA polymerase was amplified and cloned. This resulting clone was later used to create a second clone that could be induced to express his-tagged recombinant *pfu* DNA polymerase in *E. coli*. Recombinant *pfu* polymerase purified via immobilized metal ion affinity chromatography (IMAC) was produced and shown to have activity similar to that of commercially available *Pfu* DNA polymerase.

MATERIALS AND METHODS:

Bacterial Strains, Plasmids, and Enzymes:

P. furiosus genomic (DSM3638) DNA was purified and was used for PCR amplifications. *E. coli* DH5 α strain was used for preparation of plasmids and cloning, and strain BL21-CodonPlus-RIL was used for expression of the his-tagged *Pfu* DNA polymerase. *E. coli* cells were grown aerobically at 37°C in LB medium with 50 μ g/ml

ampicillin, 34 µg/ml chloramphenicol, 2% Xgal, and/or 100 mM IPTG as needed. The plasmid pGEM-T (Promega) was used for initial cloning of PCR products, and pET16-B (Novagen) was the expression vector for secondary cloning. The restriction enzyme NdeI was purchased from New England Biolabs. All other modification enzymes used were from Promega.

PCR Amplification:

The *Pfu* DNA polymerase gene was amplified using 2µg/ml of primers pfuF (5'CATATGATTTTAGATGTGGATTAC3') and pfuR (5'CGGCTCGAGTGATATCTATCGCTTTTCTAGGA3'), 1unit Promega Taq polymerase, thermophilic DNA polymerase buffer(10 mM Tris pH 9, 50 mM KCl and 0.1 Triton® X-100), 2.5 mM MgCl, 0.2 mM dNTPs, and 1.5 ng of *P. furiosus* genomic DNA. PCR products were verified by restriction enzyme digest. This same PCR reaction was also used as an assay of ligation products to confirm the presence of the *Pfu* DNA polymerase gene in the ligation products.

Cloning:

PCR products were ligated into the pGEM-T cloning vector which utilizes a single adenosine overhang for sticky-end ligation. The resulting vector, pGEM-T::pfu was then transformed into competent *E. coli* DH5α and transferred to LB plates containing Xgal, IPTG, and ampicillin. Colonies were selected for by their growth on ampicillin and screened by their ability to cleave the chromogenic substrate Xgal (Fisher). White colonies were picked, and plasmids extracted from them by Qiagen Mini-prep procedure. The fragment produced in a double digest using NdeI and XhoI of pGEM-T::pfu was ligated into pET16-B also cut with both XhoI and NdeI. This clone,

pET16-B::pfu was transformed into CaCl_2 competent *E. coli* DH5 α , plated on selective media, and screened for presence of the insert by PCR using primers used for initial gene amplification. Positive clones were then transformed into *E. coli* BL21-CodonPlus-RIL cells and plated on selective media. Clones were screened by PCR and used for protein expression.

Protein Expression and IMAC Purification:

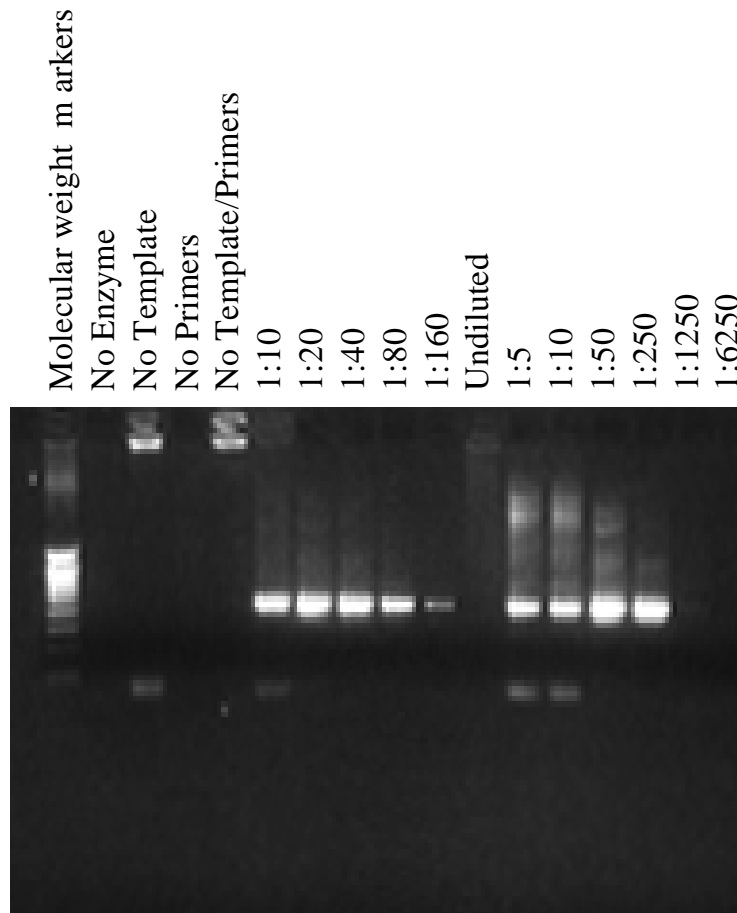
A 1 L culture of the expression host (*E. coli* BL21 codon plus) was allowed to grow to OD 0.6 upon which protein expression was induced with IPTG. *Pfu* DNA polymerase over expression was induced by adding 1 mM IPTG to a 25ml culture and optical density(OD) readings were taken over a course of 6 hours. Every hour 1 ml of culture was removed, pelleted, resuspended in protein loading dye, and analyzed by SDS-PAGE. After 6 hours the cells were pelleted and frozen. 0.16g of pelleted cells were resuspended in buffer B5 (20 mM tris pH 7.9, 500 mM NaCl, 5 mM imidazole, and 0.1% TritonX-100). This suspension was French pressed at 20,000 psi, the lysate was cleared by centrifugation, and the supernatant was transferred to a new tube. The supernatant was incubated at 75°C for half an hour and subsequently cooled on ice for 20 minutes. This suspension was centrifuged and the supernatant incubated with nickel-NTA-agarose column matrix (Qiagen). This mixture was then poured into a column and the flow through collected. The recombinant protein was then eluted with 40mM, 60mM, and 100mM imidazole buffer. This eluted protein was dialyzed in buffer containing 20mM Tris-HCl, pH 7.9, 100mM KCl, 0.1% Triton X-100, 0.1mM DTT, and 50% glycerol. Column samples were analyzed by SDS-PAGE.

Purified enzyme was used in PCR reactions to determine the dilution needed for efficient gene amplification.

RESULTS AND DISCUSSION:

PCR amplification using pfuF and pfuR produced a product of about 2400 bp, which is close to the size predicted for the amplified gene (2493bp). Cloning was successful, however there was a problem producing large amounts of pet16-B::pfu. pET16-B::pfu clones were sequenced by The University of Iowa's sequencing facility and these sequences showed *Pfu* DNA polymerase to be in the same reading frame as the upstream histidine tag. Analysis of samples taken from uninduced cultures compared to induced cultures (both containing pet16-B::pfu) showed that expression of the enzyme was dependant on induction with IPTG. SDS-PAGE analysis of the purified protein showed very little background, and large quantities of protein with a molecular weight corresponding to that reported for *Pfu* DNA polymerase. PCR amplifications showed that this protein has DNA polymerase activity although there may be some contaminating DNA retained from the host (Figure 1). (The secondary cloning, protein expression, protein purification, and the enzyme activity assays were performed by Elizabeth Haas, Mik young Ji, and Tom Hall).

Figure 1. Polymerase chain reaction assaying for polymerase activity. Each reaction contained 0.2mM dNTPs, Pfu polymerase buffer(), 2mM of forward test primer, 2mM of reverse test primer, 1ug of DNA template and 1ul of the specified polymerase. Lanes 3-5 contained commercial Taq polymerase, lanes 6-10 contained dilutions recombinant Pfu polymerase made by another lab, and lanes 11-17 contained dilutions of recombinant Pfu polymerase made using the procedure described herein. This assay was performed by Dr. Tom Hall.



REFERENCES:

Dabrowski, S. and J. Kur. 1998. Cloning and expression in *Escherichia coli* of the recombinant his-tagged DNA polymerases from *Pyrococcus furiosus* and *Pyrococcus woesei*. *Protein Expression and Purification* 15:131-138